

$B \rightarrow K^* \ell^+ \ell^-$ decay in soft-collinear effective theory

A. Ali*

*Theory Group, Deutsches Elektronen-Synchrotron DESY,
Notkestrasse 85, 22603 Hamburg, Germany.*

G. Kramer† and Guohuai Zhu‡

*II. Institut für Theoretische Physik, Universität Hamburg,
Luruper Chaussee 149, 22761 Hamburg, Germany*

(Dated: February 8, 2020)

Abstract

We study the rare B decay $B \rightarrow K^* \ell^+ \ell^-$ using soft-collinear effective theory (SCET). At leading power in $1/m_b$, a factorization formula is obtained valid to all orders in α_s . For phenomenological application, we calculate the decay amplitude including order α_s corrections, and resum the logarithms by evolving the matching coefficients from the hard scale $\mathcal{O}(m_b)$ down to the scale $\sqrt{m_b \Lambda_h}$. The branching ratio for $B \rightarrow K^* \ell^+ \ell^-$ is uncertain due to the imprecise knowledge of the soft form factors $\zeta_\perp(q^2)$ and $\zeta_\parallel(q^2)$. Constraining the soft form factor $\zeta_\perp(q^2 = 0)$ from data on $B \rightarrow K^* \gamma$ yields $\zeta_\perp(q^2 = 0) = 0.32 \pm 0.02$. Using this input, together with the light-cone sum rules to determine the q^2 dependence of $\zeta_\perp(q^2)$ and the other soft form factor $\zeta_\parallel(q^2)$, we estimate the partially integrated branching ratio in the range $1 \text{ GeV}^2 \leq q^2 \leq 7 \text{ GeV}^2$ to be $(2.92_{-0.61}^{+0.67}) \times 10^{-7}$. We discuss how to reduce the form factor related uncertainty by combining data on $B \rightarrow \rho(\rightarrow \pi\pi) \ell \nu_\ell$ and $B \rightarrow K^*(\rightarrow K\pi) \ell^+ \ell^-$. The forward-backward asymmetry is less sensitive to the input parameters. In particular, for the zero-point of the forward backward asymmetry in the standard model, we get $q_0^2 = (4.07_{-0.12}^{+0.13}) \text{ GeV}^2$.

PACS numbers: 13.25.Hw, 12.39.St, 12.38.Bx

*E-mail address: ahmed.ali@desy.de

†E-mail address: gustav.kramer@desy.de

‡E-mail address: guohuai.zhu@desy.de; Alexander-von-Humboldt Fellow

I. INTRODUCTION

The electroweak penguin decay $B \rightarrow K^*\ell^+\ell^-$ is loop-suppressed in the Standard Model(SM). It may therefore provide a rigorous test of the SM and also put strong constraints on the flavor physics beyond the SM.

Though the inclusive decay $B \rightarrow X_s\ell^+\ell^-$ is better understood theoretically using the Operator Product Expansion, and the first direct experimental measurements of the dilepton invariant mass and the m_X -distributions are already at hand [1, 2], being an inclusive process, it is extremely difficult to be measured in a hadron machine, such as the LHC, which is the only collider, except for a Super-B factory, that could provide enough luminosity for the precise study of the decay distributions of such a rare process. In contrast, for the exclusive decay $B \rightarrow K^*\ell^+\ell^-$, the difficulty lies in the imprecise knowledge of the underlying hadron dynamics. Experimentally, BaBar [3] and Belle [4] Collaborations have observed this rare decay with the branching ratios:

$$\mathcal{B}(B \rightarrow K^*\ell^+\ell^-) = \begin{cases} (16.5_{-2.2}^{+2.3} \pm 0.9 \pm 0.4) \times 10^{-7} & \text{(Belle) ,} \\ (7.8_{-1.7}^{+1.9} \pm 1.2) \times 10^{-7} & \text{(BaBar) .} \end{cases} \quad (1)$$

We note that the BELLE measurements are approximately a factor 2 higher than the corresponding BABAR measurements. In addition, BELLE has published the measurements [4, 5] of the so-called forward-backward asymmetry (FBA) [6]. In particular, the best-fit results for the Wilson coefficient ratios for negative value of A_7 ,

$$\begin{aligned} \frac{A_9}{A_7} &= -15.3_{-4.8}^{+3.4} \pm 1.1, \\ \frac{A_{10}}{A_7} &= 10.3_{-3.5}^{+5.2} \pm 1.8 , \end{aligned} \quad (2)$$

are consistent with the SM values $A_9/A_7 \simeq -13.7$ and $A_{10}/A_7 \simeq +14.9$, evaluated in the NLO approximation (see, Table I). With more data accumulated at the current B factories, and especially the huge data that will be produced at LHC, it is foreseeable that the dilepton invariant mass spectrum and the FBA in this channel will be measured precisely in several years from now, allowing a few % measurements of the Wilson coefficient ratios and the sign of A_7 .

Theoretically, the exclusive decay $B \rightarrow K^*\ell^+\ell^-$ has been studied in a number of papers, see for example [7, 8, 9, 10, 11, 12]. From the viewpoint of hadron dynamics, the application

of the QCD factorization approach [13] to this channel [14] deserves special mention. The emergence of an effective theory, called soft-collinear effective theory (SCET) [15, 16, 17, 18, 19], provides a more systematic and rigorous way to deal with the strong interaction effects of the exclusive B decays in the heavy quark expansion. For example, SCET has been used to prove the factorization of radiative $B \rightarrow V\gamma$ decays at leading power in $1/m_b$ and to all orders in α_s [20, 21]. In this paper, our aim is to improve our understanding of the strong interaction aspects in $B \rightarrow K^*\ell^+\ell^-$ decay by using SCET. Due to the similarity between $B \rightarrow K^*\gamma$ and $B \rightarrow K^*\ell^+\ell^-$ decays, our approach is quite similar to the earlier SCET-based studies [20, 21], in particular to Ref. [20].

It is well known that, when q^2 , the momentum squared of the lepton pair, is comparable to $M_{J/\psi}^2$, the resonant charmonium contributions become very important, for which there is no model-independent treatment yet. Likewise, for higher q^2 -values, higher ψ -resonances (ψ', ψ'', \dots) have to be included. Thus, in the following we will restrict ourselves to the region $1 \text{ GeV}^2 < q^2 < 7 \text{ GeV}^2$, which is dominated by short-distance contribution. Notice that the lower cut-off 1 GeV^2 is taken here because, as we shall see later, when q^2 is very soft, say $q^2 \sim \mathcal{O}(\Lambda_{QCD}^2)$, the factorization of the annihilation topology breaks down.

In this kinematic region, the following factorization formula for the decay amplitude, which holds to all orders in α_s at the leading power in $1/m_b$, can be derived in SCET:

$$\langle K_a^*\ell^+\ell^- | H_{eff} | B \rangle = T_a^I \zeta_a(q^2) + \sum_{\pm} \int_0^{\infty} \frac{d\omega}{\omega} \phi_{B,\pm}(\omega) \int_0^1 du \phi_{K^*,a}(u) T_{a,\pm}^{II}(\omega, u) \quad (3)$$

where $a = \parallel, \perp$ denotes the polarization of the K^* meson. The functions T^I and T^{II} are perturbatively calculable. $\zeta_a(q^2)$ are the soft form factors defined in SCET while $\phi_{B,\pm}$ and $\phi_{K^*,a}$ are the light-cone distribution amplitudes (LCDAs) for the B and K^* mesons, respectively. Compared to the earlier results of Ref. [14], obtained in the large-energy limit of QCD, the main phenomenological improvement is that for the hard scattering function T^{II} , the perturbative logarithms are summed from the hard scale $\mu_b \sim \mathcal{O}(m_b)$ down to the intermediate scale $\sqrt{\mu_b \Lambda_h}$, where Λ_h represents a typical hadronic scale. Notice also that the definitions of the soft form factors ζ_a in SCET are different from those of Ref. [14], therefore the explicit expressions for T^I are also different in the two approaches.

This paper is organized as follows: In section II, we briefly review the basic ideas and notations of SCET. We then list the relevant effective operators in SCET and do the explicit matching calculations from QCD to SCET_I (Sec. II A) and from SCET_I to SCET_{II} (Sec. II

B). The matrix elements of the effective SCET operators are given in Sec. II C. At the end of this section, the logarithmic resummation in SCET_I is discussed. In section III, we consider the phenomenological aspects of $B \rightarrow K^* \ell^+ \ell^-$ decay. We first specify the input parameters, especially the soft form factors $\zeta_{\perp, \parallel}(q^2)$ (Sec. III A), which are the cause of the largest theoretical uncertainty. We use the q^2 -dependence of the related QCD form factors in the LC-QCD sum rule approach, but fix the normalization of these soft form factors using constraints from data on the exclusive decays $B \rightarrow K^* \gamma$. In Sec. III B, we work out numerically the evolution of the B-type SCET_I matching coefficients, defined earlier in Sec. II. We then give the dilepton invariant mass spectrum and the forward-backward asymmetry in the decay $B \rightarrow K^* \ell^+ \ell^-$, and compare the integrated branching ratios with the measurements from BaBar and Belle (Sec. III C). We end with a summary of our results in section IV and suggestions of future measurements to reduce the model dependence due to the form factors and other input parameters.

II. SCET ANALYSIS OF $B \rightarrow K^* \ell^+ \ell^-$

For the $b \rightarrow s$ transitions, the weak effective Hamiltonian can be written as

$$H_{eff} = -\frac{G_F}{\sqrt{2}} V_{ts}^* V_{tb} \sum_{i=1}^{10} C_i(\mu) Q_i(\mu), \quad (4)$$

where we have neglected the contribution proportional to $V_{us}^* V_{ub}$ in the penguin (loop) amplitudes, which is doubly Cabibbo-suppressed, and have used the unitarity of the CKM matrix to factorize the overall CKM-matrix element dependence. We use the operator basis introduced in [14, 23]:

$$\begin{aligned} Q_1 &= (\bar{s} T^A c)_{V-A} (\bar{c} T^A b)_{V-A}, & Q_2 &= (\bar{s} c)_{V-A} (\bar{c} b)_{V-A}, \\ Q_3 &= 2 (\bar{s} b)_{V-A} \sum_q (\bar{q} \gamma^\mu q), & Q_4 &= 2 (\bar{s} T^A b)_{V-A} \sum_q (\bar{q} \gamma^\mu T^A q), \\ Q_5 &= 2 \bar{s} \gamma_\mu \gamma_\nu \gamma_\rho (1 - \gamma_5) b \sum_q (\bar{q} \gamma^\mu \gamma^\nu \gamma^\rho q), & & \\ Q_6 &= 2 \bar{s} \gamma_\mu \gamma_\nu \gamma_\rho (1 - \gamma_5) T^A b \sum_q (\bar{q} \gamma^\mu \gamma^\nu \gamma^\rho T^A q), & & \\ Q_7 &= -\frac{g_{em} \bar{m}_b}{8\pi^2} \bar{s} \sigma^{\mu\nu} (1 + \gamma_5) b F_{\mu\nu}, & Q_8 &= -\frac{g_s \bar{m}_b}{8\pi^2} \bar{s} \sigma^{\mu\nu} (1 + \gamma_5) T^A b G_{\mu\nu}^A, \\ Q_9 &= \frac{\alpha_{em}}{2\pi} (\bar{s} b)_{V-A} (\bar{\ell} \gamma^\mu \ell), & Q_{10} &= \frac{\alpha_{em}}{2\pi} (\bar{s} b)_{V-A} (\bar{\ell} \gamma^\mu \gamma_5 \ell), \end{aligned} \quad (5)$$

where T^A is the SU(3) color matrix, $\alpha_{em} = g_{em}^2/4\pi$ is the fine-structure constant and $\overline{m}_b(\mu)$ the current mass of the b quark in the \overline{MS} scheme at the scale μ .

Restricting ourselves to the kinematic region $1 \text{ GeV}^2 < q^2 < 7 \text{ GeV}^2$, the light K^* meson moves fast with large momentum of the order of $m_B/2$, which thus can be viewed approximately as a collinear particle. For convenience, let us assume that the K^* meson is moving in the direction of the light-like reference vector n , then its momentum can be decomposed as $p = \bar{n} \cdot pn/2 + p_\perp + n \cdot p\bar{n}/2$, where \bar{n} is another light-like reference vector satisfying $n \cdot \bar{n} = 2$. In this light-cone frame, the collinear momentum of K^* is expressed as

$$p = (n \cdot p, \bar{n} \cdot p, p_\perp) \sim (\lambda^2, 1, \lambda)m_b, \quad (6)$$

with $\lambda \sim \Lambda/m_b \ll 1$. In addition to this collinear mode, the soft and hard-collinear modes, with momenta scaling as $(\lambda, \lambda, \lambda)m_b$ and $(\lambda, 1, \sqrt{\lambda})m_b$, respectively, are also necessary to correctly reproduce the infrared behavior of full QCD.

SCET introduces fields for every momentum mode and we will encounter the following quark and gluon fields

$$\begin{aligned} \xi_c \sim \lambda, \quad A_c^\mu \sim (\lambda^2, 1, \lambda), \quad \xi_{hc} \sim \lambda^{1/2}, \quad A_{hc}^\mu \sim (\lambda, 1, \lambda^{1/2}), \\ q_s \sim \lambda^{3/2}, \quad A_s^\mu \sim (\lambda, \lambda, \lambda), \quad h \sim \lambda^{3/2}, \end{aligned} \quad (7)$$

where we have made their scale-dependence explicit. In the above, the symbol A^μ stands for the gluon field, h represents a heavy quark field, the symbols ξ and q stand for the light quark fields, and the subscripts c, s, hc stand for collinear, soft and hard collinear modes, respectively. Note that in this paper, the momentum q of the lepton pair is taken formally as a hard momentum, though numerically in the range $1 \text{ GeV}^2 < q^2 < 7 \text{ GeV}^2$ it is more like a hard collinear momentum. This treatment simplifies a little bit the SCET derivation in that we do not need to introduce an extra hard collinear mode in the \bar{n} direction. As explained in detail in Ref. [20], to construct the gauge invariant operators in SCET, it is more convenient to introduce the building blocks, given below, which are obtained by multiplying the fields by the Wilson lines which run along the light-ray to infinity:

$$\mathcal{X}_c, \quad A_c^\mu, \quad \mathcal{X}_{hc}, \quad A_{hc}^\mu, \quad \mathcal{Q}_s, \quad A_s^\mu, \quad \mathcal{H}_s. \quad (8)$$

For example, the field \mathcal{X}_{hc} is defined as

$$\mathcal{X}_{hc}(x) = W_{hc}^\dagger(x) \xi_{hc}(x); \quad \text{with } W_{hc}(x) = P \exp \left(ig \int_{-\infty}^0 ds \bar{n} \cdot A_{hc}(x + s\bar{n}) \right), \quad (9)$$

where $W_{hc}(x)$ is a hard collinear Wilson line. For the definitions of the other fields and more technical details about SCET, we refer the reader to Ref. [20] and references therein.

Since SCET contains two collinear fields, *i.e.* hard collinear and collinear fields, normally an intermediate effective theory, called SCET_I, is introduced which contains only soft and hard collinear fields. While the final effective theory, called SCET_{II}, contains only soft and collinear fields. We will then do a two-step matching from $QCD \rightarrow SCET_I \rightarrow SCET_{II}$.

A. QCD to SCET_I matching

In SCET_I, the K^* meson is taken as a hard collinear particle and the relevant building blocks are \mathcal{X}_{hc} , \mathcal{A}_{hc}^μ , \mathcal{Q}_s , \mathcal{A}_s^μ and \mathcal{H}_s . The velocity of the B meson is defined as $v = P_B/m_B$. The matching from QCD to SCET_I at leading power may be expressed as

$$H_{eff} \rightarrow -\frac{G_F}{\sqrt{2}} V_{ts}^* V_{tb} \left(\sum_{i=1}^4 \int ds \tilde{C}_i^A(s) J_i^A(s) + \sum_{j=1}^4 \int ds \int dr \tilde{C}_j^B(s, r) J_j^B(s, r) + \int ds \int dr \int dt \tilde{C}^C(s, r, t) J^C(s, r, t) \right), \quad (10)$$

where $\tilde{C}_i^{(A,B,C)}$ are Wilson coefficients in position space. The relevant SCET_I operators for $B \rightarrow K^* \ell^+ \ell^-$ decay are constructed by using the building blocks mentioned above [20]:

$$\begin{aligned} J_1^A &= \bar{\mathcal{X}}_{hc}(s\bar{n})(1 + \gamma_5)\gamma_\perp^\mu h(0) \bar{\ell}\gamma_\mu \ell, & J_2^A &= \bar{\mathcal{X}}_{hc}(s\bar{n})(1 + \gamma_5)\frac{n^\mu}{n \cdot v} h(0) \bar{\ell}\gamma_\mu \ell, \\ J_3^A &= \bar{\mathcal{X}}_{hc}(s\bar{n})(1 + \gamma_5)\gamma_\perp^\mu h(0) \bar{\ell}\gamma_\mu \gamma_5 \ell, & J_4^A &= \bar{\mathcal{X}}_{hc}(s\bar{n})(1 + \gamma_5)\frac{n^\mu}{n \cdot v} h(0) \bar{\ell}\gamma_\mu \gamma_5 \ell, \\ J_1^B &= \bar{\mathcal{X}}_{hc}(s\bar{n})(1 + \gamma_5)\gamma_\perp^\mu \mathcal{A}_{hc\perp}(r\bar{n})h(0) \bar{\ell}\gamma_\mu \ell, \\ J_2^B &= \bar{\mathcal{X}}_{hc}(s\bar{n})(1 + \gamma_5)\mathcal{A}_{hc\perp}(r\bar{n})\frac{n^\mu}{n \cdot v} h(0) \bar{\ell}\gamma_\mu \ell, & (11) \\ J_3^B &= \bar{\mathcal{X}}_{hc}(s\bar{n})(1 + \gamma_5)\gamma_\perp^\mu \mathcal{A}_{hc\perp}(r\bar{n})h(0) \bar{\ell}\gamma_\mu \gamma_5 \ell, \\ J_4^B &= \bar{\mathcal{X}}_{hc}(s\bar{n})(1 + \gamma_5)\mathcal{A}_{hc\perp}(r\bar{n})\frac{n^\mu}{n \cdot v} h(0) \bar{\ell}\gamma_\mu \gamma_5 \ell, \\ J^C &= \bar{\mathcal{X}}_{hc}(s\bar{n})(1 + \gamma_5)\frac{\not{r}}{2}\mathcal{X}_{hc}(r\bar{n})\bar{\mathcal{Q}}_{\bar{s}}(t\bar{n})(1 + \gamma_5)\frac{\not{r}}{2}\frac{n^\mu}{n \cdot v} h(0) \bar{\ell}\gamma_\mu \ell, \end{aligned}$$

where the operators J_i^A and J_j^B represent the cases that the lepton pair is emitted from the $b \rightarrow s$ transition currents, while J^C represents the weak annihilation terms in which the lepton pair is emitted from the spectator quark of the B meson. Except the lepton pair, the operators $J^{(A,B)}$ have the same Dirac structures as those of the heavy-to-light transition

currents in SCET, which were first derived in Ref. [16] for J_i^A and in Refs. [24, 25] for J_j^B . In this paper we take the operator basis of [20, 25] which makes J^B multiplicatively renormalized, but we have neglected the operators which contain the Dirac structure $\mathcal{A}_{hc\perp}\gamma_\perp^\mu$ and which do not contribute to the B meson decays. It is also clear that the structure $\bar{\ell}\gamma_\mu\gamma_5\ell$ arises solely from Q_{10} of the weak effective Hamiltonian.

Since in practice the matching calculations are done in momentum space, it is more convenient to define the Wilson coefficients in momentum space by the following Fourier-transformations:

$$\begin{aligned} C_i^A(E) &= \int ds e^{is\bar{n}\cdot P} \tilde{C}_i^A(s) , \\ C_j^B(E, u) &= \int ds \int dr e^{i(us+\bar{u}r)\bar{n}\cdot P} \tilde{C}_j^B(s, r) , \\ C^C(E, u, \omega) &= \int ds \int dr \int dt e^{i(us+\bar{u}r)\bar{n}\cdot P} e^{-i\omega\bar{n}\cdot vt} \tilde{C}^C(s, r, t) , \end{aligned} \quad (12)$$

with $E \equiv n \cdot v\bar{n} \cdot P/2$ and $\bar{u} = 1 - u$. To get the order α_s corrections to the decay amplitude, we need to calculate the Wilson coefficients C_i^A to one-loop level and $C_j^{(B,C)}$ to tree level. In the following we will use $\Delta_j C_i^{(A,B,C)}$ to denote the matching results from the weak effective operators Q_j to the SCET current $J_i^{(A,B,C)}$. With this, the matching coefficients from $QCD \rightarrow SCET_I$ can be written as

$$C_i^{(A,B,C)} = \sum_{j=1}^{10} \Delta_j C_i^{(A,B,C)}(\mu_{QCD}, \mu) , \quad (13)$$

where μ_{QCD} is the matching scale and μ the renormalization scale in $SCET_I$.

Each operator of the weak effective Hamiltonian, namely Q_{1-10} , will contribute to C_i^A at order α_s level, as shown in Fig. 1. But due to the small Wilson coefficients C_{3-6} , it is numerically reasonable to neglect the contributions from Q_{3-6} . For the operators $Q_{1,2}$ and Q_8 , the results can be easily derived from Eqs. (11) and (25) of Ref. [26]:

$$\begin{aligned} \Delta_{1,2} C_1^A(\mu_{QCD}) &= -\frac{\alpha_{em}}{2\pi} \frac{\alpha_s(\mu_{QCD})}{4\pi} \left[\frac{1}{\hat{s}} (2F_2^{(7)} + \hat{s}F_2^{(9)}) \bar{C}_2 + 2(F_1^{(9)} + F_2^{(9)}/6) \bar{C}_1 \right] , \\ \Delta_{1,2} C_2^A(\mu_{QCD}) &= -\frac{\alpha_{em}}{2\pi} \frac{\alpha_s(\mu_{QCD})}{4\pi} \left[(2F_2^{(7)} + F_2^{(9)}) \bar{C}_2 + 2(F_1^{(9)} + F_2^{(9)}/6) \bar{C}_1 \right] , \\ \Delta_8 C_1^A(\mu_{QCD}) &= -\frac{\alpha_{em}}{2\pi} \frac{\alpha_s(\mu_{QCD})}{4\pi} \frac{\bar{m}_b(\mu_{QCD})}{m_b} \left[\frac{2}{\hat{s}} F_8^{(7)} + F_8^{(9)} \right] C_8^{eff} , \\ \Delta_8 C_2^A(\mu_{QCD}) &= -\frac{\alpha_{em}}{2\pi} \frac{\alpha_s(\mu_{QCD})}{4\pi} \frac{\bar{m}_b(\mu_{QCD})}{m_b} \left[2F_8^{(7)} + F_8^{(9)} \right] C_8^{eff} , \end{aligned} \quad (14)$$

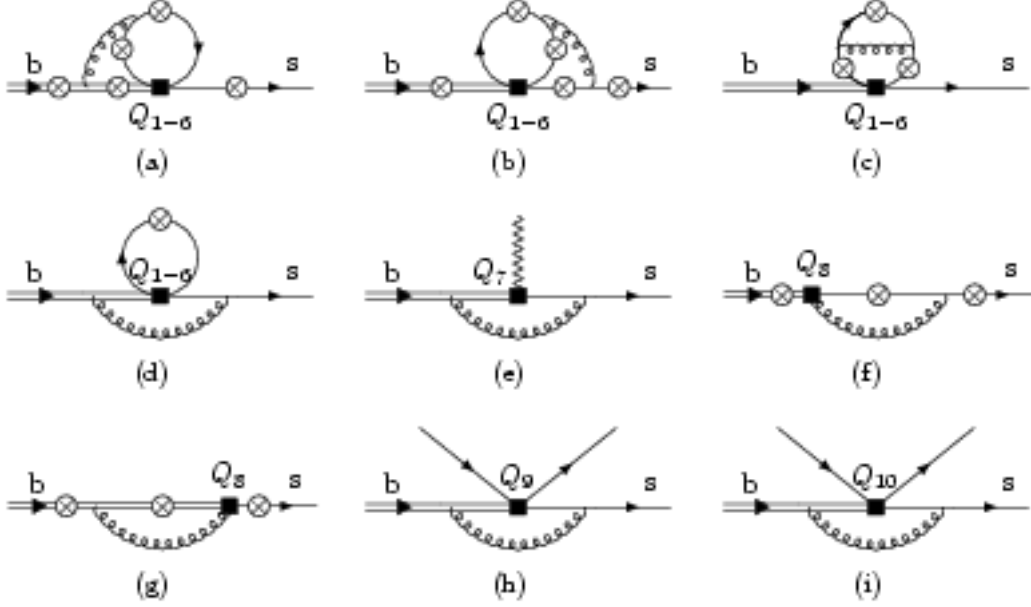


FIG. 1: $\mathcal{O}(\alpha_s)$ contributions to the matching of Q_i to A-type SCET currents. The crossed circles denote the possible locations from where the virtual photon is emitted and then splits into a lepton pair.

where $\hat{s} \equiv q^2/m_b^2$ and m_b is the pole mass of the b quark. The current mass \bar{m}_b is related to the pole mass at next-to-leading order by

$$\bar{m}_b(\mu) = m_b \left[1 + \frac{\alpha_s C_F}{4\pi} \left(3 \ln \frac{m_b^2}{\mu^2} - 4 \right) \right], \quad (15)$$

where $C_F = 4/3$. The functions $F_{1,2,8}^{(7,9)}$ are given in a mixed analytic and numerical form in Ref. [26]. Following the convention of Ref. [14], we also use the "barred" coefficients \bar{C}_i ($i=1, \dots, 6$) here which are the linear combinations of the Wilson coefficients C_i of the weak effective Hamiltonian in Eq. (4). The effective Wilson coefficient C_8^{eff} is defined as $C_8^{eff} = C_8 + C_3 - C_4/6 + 20C_5 - 10C_6$.

For the operators Q_7 , Q_9 and Q_{10} , the matchings to the A-type currents give

$$\begin{aligned} \Delta_7 C_1^A &= \frac{\alpha_{em} \bar{m}_b(\mu_{\text{QCD}})}{2\pi} \frac{2}{m_b} \frac{\tilde{C}_9}{\hat{s}} C_7^{eff}, & \Delta_7 C_2^A &= \frac{\alpha_{em} \bar{m}_b(\mu_{\text{QCD}})}{2\pi} \frac{2\tilde{C}_{10}}{m_b} C_7^{eff}, \\ \Delta_9 C_1^A &= \frac{\alpha_{em}}{2\pi} \tilde{C}_3 C_9^{eff}, & \Delta_9 C_2^A &= \frac{\alpha_{em}}{2\pi} \left(\tilde{C}_4 + \frac{1-\hat{s}}{2} \tilde{C}_5 \right) C_9^{eff}, \\ \Delta_{10} C_3^A &= \frac{\alpha_{em}}{2\pi} \tilde{C}_3 C_{10}, & \Delta_{10} C_4^A &= \frac{\alpha_{em}}{2\pi} \left(\tilde{C}_4 + \frac{1-\hat{s}}{2} \tilde{C}_5 \right) C_{10}. \end{aligned} \quad (16)$$

To avoid confusion with the Wilson coefficients in Eq. (4), we use the notations \tilde{C}_i for the

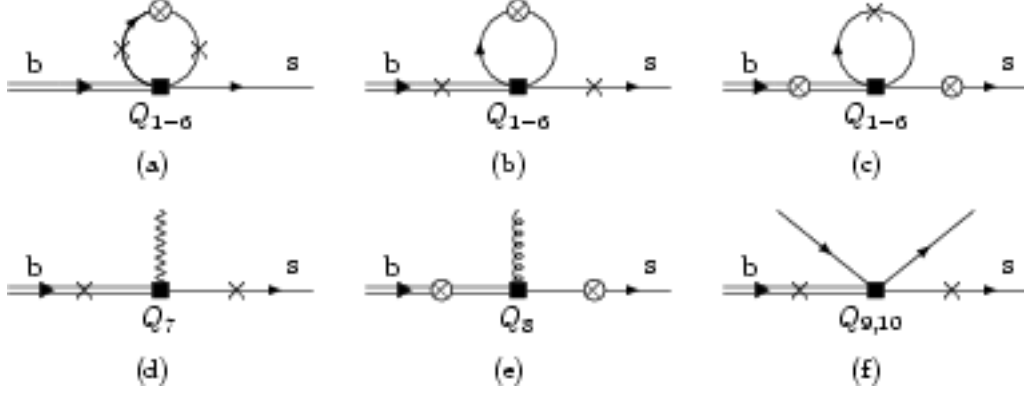


FIG. 2: Tree-level matching of Q_i onto B-type SCET currents. The crossed circles denote the possible locations from where the virtual photon is emitted, while the crosses mark the possible places where a gluon line may be attached.

matching coefficients, instead of C_i used originally in Ref. [16]. The explicit expressions of \tilde{C}_i up to one-loop order can be read from [16, 24]. Note that although the operator basis of the tensor current in [24] looks slightly different from that of [16], they are actually the same and it is easy to find the relations $\tilde{C}_9 = C_T^{(A0)2}$ and $\tilde{C}_{10} = C_T^{(A0)1}$. The effective Wilson coefficients are defined as $C_7^{eff} = C_7 - C_3/3 - 4C_4/9 - 20C_5/3 - 80C_6/9$ and $C_9^{eff} = C_9 + Y(q^2)$ where the function $Y(q^2)$ represents the contributions of the fermion loops and the explicit formula can be found in [14].

To get the decay amplitude of $B \rightarrow K^* \ell^+ \ell^-$ in order α_s , the tree level matching of the effective weak Hamiltonian onto B-type SCET currents is already enough, as illustrated in Fig. 2. If we use the notation $\Delta_{16} C_i^B$ to stand for the matchings of Q_{1-6} onto B-type SCET current J_i^B , namely $\Delta_{16} C_i^B \equiv \sum_{j=1}^6 \Delta_j C_i^B$, we get from Fig. 2a that

$$\begin{aligned} \Delta_{16} C_1^B &= -\frac{\alpha_{em}}{2\pi} \frac{1}{m_b \hat{s}} \left(\frac{2}{3} F_{16}^\perp(u, \hat{s}, m_c^2/m_b^2) (\bar{C}_2 + \bar{C}_4 - \bar{C}_6) - \frac{1}{3} F_{16}^\perp(u, \hat{s}, 0) \bar{C}_3 - \right. \\ &\quad \left. \frac{1}{3} F_{16}^\perp(u, \hat{s}, 1) (\bar{C}_3 + \bar{C}_4 - \bar{C}_6 - 4\bar{C}_5) \right), \\ \Delta_{16} C_2^B &= \frac{\alpha_{em}}{2\pi} \frac{2}{m_b} \left(\frac{2}{3} F_{16}^\parallel(u, \hat{s}, m_c^2/m_b^2) (\bar{C}_2 + \bar{C}_4 - \bar{C}_6) - \frac{1}{3} F_{16}^\parallel(u, \hat{s}, 0) \bar{C}_3 - \right. \\ &\quad \left. \frac{1}{3} F_{16}^\parallel(u, \hat{s}, 1) (\bar{C}_3 + \bar{C}_4 - \bar{C}_6) \right), \end{aligned} \tag{17}$$

where u is the momentum fraction carried by the strange quark of the K^* meson. The

functions $F_{16}^{\perp,\parallel}$ are defined as

$$\begin{aligned}
F_{16}^{\perp}(u, \hat{s}, \lambda) = & 1 + \frac{2}{(1-\hat{s})(1-u)} \left(\hat{s} \left(\frac{\sqrt{-\hat{s}+4\lambda}}{\sqrt{\hat{s}}} \arctan \frac{\sqrt{\hat{s}}}{\sqrt{-\hat{s}+4\lambda}} - \right. \right. \\
& \frac{\sqrt{-1+u-\hat{s}u+4\lambda}}{\sqrt{1-(1-\hat{s})u}} \arctan \frac{\sqrt{1-(1-\hat{s})u}}{\sqrt{-1+u-\hat{s}u+4\lambda}} \left. \left. + \lambda \operatorname{Li}_2 \left(\frac{2\sqrt{\hat{s}}}{\sqrt{\hat{s}}-\sqrt{\hat{s}-4\lambda}} \right) \right) \right. \\
& + \lambda \operatorname{Li}_2 \left(\frac{2\sqrt{\hat{s}}}{\sqrt{\hat{s}}+\sqrt{\hat{s}-4\lambda}} \right) - \lambda \operatorname{Li}_2 \left(\frac{2\sqrt{1-(1-\hat{s})u}}{\sqrt{1-(1-\hat{s})u}+\sqrt{1-(1-\hat{s})u-4\lambda}} \right) \\
& \left. - \lambda \operatorname{Li}_2 \left(\frac{2\sqrt{1-(1-\hat{s})u}}{\sqrt{1-(1-\hat{s})u}-\sqrt{1-(1-\hat{s})u-4\lambda}} \right) \right), \tag{18}
\end{aligned}$$

$$\begin{aligned}
F_{16}^{\parallel}(u, \hat{s}, \lambda) = & 2\hat{s} + \frac{4\hat{s}}{(1-\hat{s})(1-u)} \left((1-u+u\hat{s}) \left(\frac{\sqrt{-\hat{s}+4\lambda}}{\sqrt{\hat{s}}} \arctan \frac{\sqrt{\hat{s}}}{\sqrt{-\hat{s}+4\lambda}} - \right. \right. \\
& \frac{\sqrt{-1+u-\hat{s}u+4\lambda}}{\sqrt{1-(1-\hat{s})u}} \arctan \frac{\sqrt{1-(1-\hat{s})u}}{\sqrt{-1+u-\hat{s}u+4\lambda}} \left. \left. + \lambda \operatorname{Li}_2 \left(\frac{2\sqrt{\hat{s}}}{\sqrt{\hat{s}}-\sqrt{\hat{s}-4\lambda}} \right) \right) \right. \\
& + \lambda \operatorname{Li}_2 \left(\frac{2\sqrt{\hat{s}}}{\sqrt{\hat{s}}+\sqrt{\hat{s}-4\lambda}} \right) - \lambda \operatorname{Li}_2 \left(\frac{2\sqrt{1-(1-\hat{s})u}}{\sqrt{1-(1-\hat{s})u}+\sqrt{1-(1-\hat{s})u-4\lambda}} \right) \\
& \left. - \lambda \operatorname{Li}_2 \left(\frac{2\sqrt{1-(1-\hat{s})u}}{\sqrt{1-(1-\hat{s})u}-\sqrt{1-(1-\hat{s})u-4\lambda}} \right) \right). \tag{19}
\end{aligned}$$

As a check, it is not difficult to find the following relations

$$F_{16}^{\perp}(u, \hat{s}, \lambda) = t_{\perp}(u, m_q) \times \frac{(1-u)E}{2M_B}, \quad F_{16}^{\parallel}(u, \hat{s}, \lambda) = t_{\parallel}(u, m_q) \times \frac{\hat{s}(1-u)E}{M_B},$$

where the functions $t_{\perp,\parallel}(u, m_q)$ are defined in Eqs. (27)-(28) in the paper by Beneke *et al.* [14].

We also note that the functions $F_{16}^{\perp}(u, \hat{s}, \lambda)$ and $F_{16}^{\parallel}(u, \hat{s}, \lambda)$ are finite as $\bar{u} = 1-u \rightarrow 0$, as opposed to the functions $t_{\perp,\parallel}(u, m_q)$, which are singular as $\bar{u} \rightarrow 0$.

Fig. 2d and the operator Q_9 of Fig. 2f, combined with Fig. 2b, will contribute to the matching coefficients $\Delta_{7,9}C_{1,2}^B$, while the operator Q_{10} of Fig. 2f will contribute to $\Delta_{10}C_{3,4}^B$:

$$\begin{aligned}
\Delta_7 C_1^B &= -\frac{\alpha_{em}}{2\pi} \frac{\bar{m}_b}{m_b^2 \hat{s}} 2C_7^{eff}, & \Delta_7 C_2^B &= \frac{\alpha_{em}}{2\pi} \frac{\bar{m}_b}{m_b^2 (1-\hat{s})} 2C_7^{eff}, \\
\Delta_9 C_1^B &= 0, & \Delta_9 C_2^B &= -\frac{\alpha_{em}}{2\pi} \frac{1-2\hat{s}}{m_b (1-\hat{s})} C_9^{eff}, \\
\Delta_{10} C_3^B &= 0, & \Delta_{10} C_4^B &= -\frac{\alpha_{em}}{2\pi} \frac{1-2\hat{s}}{m_b (1-\hat{s})} C_{10}.
\end{aligned} \tag{20}$$

Finally, Fig. 2e together with Fig. 2c contribute to the matching coefficients

$$\Delta_8 C_1^B = -\frac{\alpha_{em}}{2\pi} \frac{\bar{m}_b}{m_b^2} \frac{2(1-u)(1-\hat{s})}{3\hat{s}(u+\hat{s}-u\hat{s})} C_8^{eff}, \quad \Delta_8 C_2^B = 0. \tag{21}$$

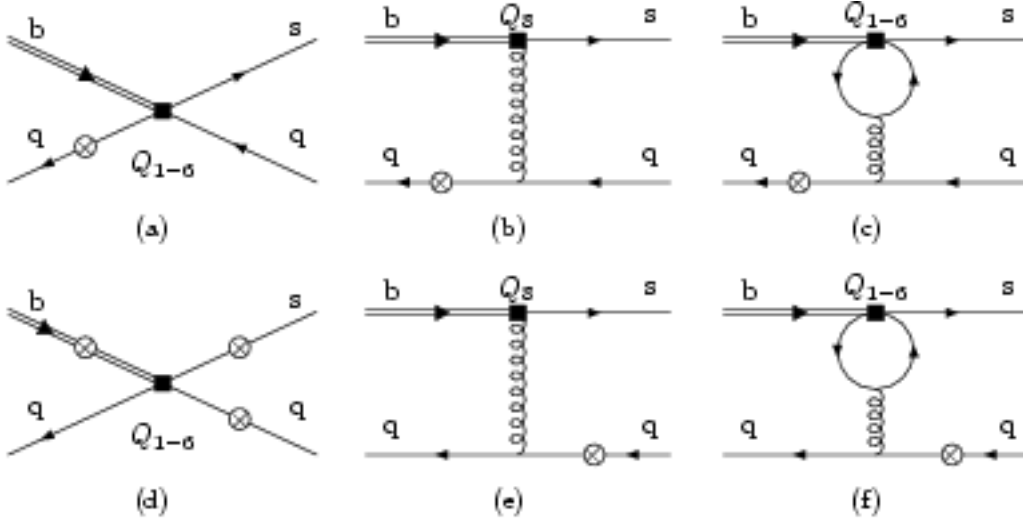


FIG. 3: The annihilation topology where the virtual photon is emitted from the spectator quark denoted by the crossed circle.

We shall now consider the annihilation topology where the virtual (off-shell) photon is emitted from the spectator quark, as shown in Fig. 3. Due to the off-shellness of the quark propagator, it is easy to check that Fig. (3d-3f) are of order $1/m_b$ suppressed compared with Fig. (3a-3c) where the photon is emitted from the spectator quark in the B meson. Therefore at leading power in $1/m_b$, only the first three diagrams in Fig. 3 are relevant for our analysis. As we shall see in the following, all of these three diagrams contribute to the C-type SCET current.

The annihilation topology, Fig. 3a, contributes to the matching coefficient at order α_s^0 , for which the calculation is trivial,

$$\Delta_{16}^{(0)} C^C = \frac{16\pi^2}{3} \frac{\alpha_{em}}{2\pi} \frac{e_q}{e} \frac{1}{m_b(m_b\omega - q^2 - i\epsilon)} \left(-\frac{V_{us}^* V_{ub}}{V_{ts}^* V_{tb}} (\bar{C}_1 + 3\bar{C}_2) \delta_{qu} + (\bar{C}_3 + 3\bar{C}_4) \right). \quad (22)$$

Here e_q is the electric charge of the spectator quark in the B meson and the superscript (0) denotes the matching at order α_s^0 . At order α_s , Fig. (3b-3c) also contribute to the matching

onto C-type SCET current with the coefficients

$$\begin{aligned}
\Delta_8 C^C &= 8\pi^2 \frac{\alpha_{em} e_q}{2\pi} \frac{1}{e m_b(m_b\omega - q^2 - i\epsilon)} \frac{C_F \alpha_s}{N_c 4\pi} \frac{-4C_8^{eff}}{1 - u + u\hat{s}} , \\
\Delta_{16}^{(1)} C^C &= 16\pi^2 \frac{\alpha_{em} e_q}{2\pi} \frac{1}{e m_b(m_b\omega - q^2 - i\epsilon)} \frac{C_F \alpha_s}{N_c 4\pi} \left\{ (\bar{C}_2 + \bar{C}_4 + \bar{C}_6)G(u, \hat{s}, m_c^2/m_b^2) + \right. \\
&\quad (\bar{C}_3 + 3\bar{C}_4 + 3\bar{C}_6)G(u, \hat{s}, 0) + (\bar{C}_3 + \bar{C}_4 + \bar{C}_6)G(u, \hat{s}, 1) + \\
&\quad \left. \frac{4}{9}(\bar{C}_3 - \bar{C}_5 - 15\bar{C}_6) \right\} , \tag{23}
\end{aligned}$$

with the function $G(u, \hat{s}, \lambda)$ defined as

$$G(u, \hat{s}, \lambda) = \frac{2}{3} + \frac{2}{3} \ln \frac{m_b^2}{\mu^2} + 4 \int_0^1 dx x(1-x) \ln[\lambda - x(1-x)(1-u+u\hat{s})] . \tag{24}$$

For later convenience, we will introduce $\Delta_i \hat{C}^C \equiv \Delta_i C^C \times (\omega - q^2/m_b)$.

B. SCET_I → SCET_{II} matching

As shown in Ref. [27], which analyzes the form factors in the framework of SCET, one may simply define the matrix elements of the A-type SCET_I currents as non-perturbative input since the non-factorizable part of the form factors are all contained in such matrix elements. Therefore the explicit matching of J^A to SCET_{II} is not necessary here.

For B-type SCET_I operators, they are matched onto the following SCET_{II} operators

$$\begin{aligned}
O_1^B &= \bar{\mathcal{X}}_c(s\bar{n})(1 + \gamma_5)\gamma_\perp^\mu \frac{\not{n}}{2} \mathcal{X}_c(0) \bar{\mathcal{Q}}_s(tn)(1 - \gamma_5) \frac{\not{n}}{2} \mathcal{H}_s(0) \bar{\ell}\gamma_\mu \ell , \\
O_2^B &= \bar{\mathcal{X}}_c(s\bar{n})(1 + \gamma_5) \frac{n^\mu}{n \cdot v} \frac{\not{n}}{2} \mathcal{X}_c(0) \bar{\mathcal{Q}}_s(tn)(1 + \gamma_5) \frac{\not{n}}{2} \mathcal{H}_s(0) \bar{\ell}\gamma_\mu \ell , \\
O_3^B &= \bar{\mathcal{X}}_c(s\bar{n})(1 + \gamma_5)\gamma_\perp^\mu \frac{\not{n}}{2} \mathcal{X}_c(0) \bar{\mathcal{Q}}_s(tn)(1 - \gamma_5) \frac{\not{n}}{2} \mathcal{H}_s(0) \bar{\ell}\gamma_\mu \gamma_5 \ell , \\
O_4^B &= \bar{\mathcal{X}}_c(s\bar{n})(1 + \gamma_5) \frac{n^\mu}{n \cdot v} \frac{\not{n}}{2} \mathcal{X}_c(0) \bar{\mathcal{Q}}_s(tn)(1 + \gamma_5) \frac{\not{n}}{2} \mathcal{H}_s(0) \bar{\ell}\gamma_\mu \gamma_5 \ell , \tag{25}
\end{aligned}$$

where we only include the color-singlet operators that have non-zero matrix elements for the $B \rightarrow K^* \ell^+ \ell^-$ decay. Again, it is in practice more convenient to do the matching calculations in momentum space, and the Wilson coefficients can be defined by Fourier transforming the corresponding ones in position space, just like the case in SCET_I,

$$D_i^B(\omega, u) = \int ds \int dt e^{-i\omega n \cdot vt} e^{ius\bar{n} \cdot P} \tilde{D}_i^B(s, t). \tag{26}$$

Following the notations of [20], the Wilson coefficients D_i^B can be expressed as

$$D_i^B(\omega, u, \mu) = \frac{1}{\omega} \int_0^1 dy \mathcal{J}_i \left(u, v, \ln \frac{m_b \omega (1 - \hat{s})}{\mu^2}, \mu \right) C_i^B(v, \mu), \quad (27)$$

where the jet functions \mathcal{J}_i arise from the SCET_I \rightarrow SCET_{II} matching and it is clear that $\mathcal{J}_1 = \mathcal{J}_3 \equiv \mathcal{J}_\perp$ and $\mathcal{J}_2 = \mathcal{J}_4 \equiv \mathcal{J}_\parallel$. At tree level, using the Fierz-transformation in the operator basis,

$$\begin{aligned} \bar{\mathcal{X}}_c N \mathcal{H}_s \bar{\mathcal{Q}}_s M \mathcal{X}_c &= -\frac{1}{4} \bar{\mathcal{X}}_c (1 + \gamma_5) \frac{\not{h}}{2} \mathcal{X}_c \bar{\mathcal{Q}}_s M (1 - \gamma_5) \frac{\not{h}}{2} N \mathcal{H}_s - \frac{1}{4} \bar{\mathcal{X}}_c (1 - \gamma_5) \frac{\not{h}}{2} \mathcal{X}_c \\ &\quad \bar{\mathcal{Q}}_s M (1 + \gamma_5) \frac{\not{h}}{2} N \mathcal{H}_s - \frac{1}{8} \bar{\mathcal{X}}_c (1 + \gamma_5) \frac{\not{h}}{2} \gamma_{\perp\alpha} \mathcal{X}_c \bar{\mathcal{Q}}_s M (1 + \gamma_5) \gamma_{\perp}^\alpha \frac{\not{h}}{2} N \mathcal{H}_s, \end{aligned} \quad (28)$$

one obtains

$$\mathcal{J}_\perp(u, v) = \mathcal{J}_\parallel(u, v) = -\frac{4\pi C_F \alpha_s}{N_c} \frac{1}{m_b(1-u)(1-\hat{s})} \delta(u-v). \quad (29)$$

Finally, for the C-type SCET_I current, it will be matched onto the operator

$$O^C = \bar{\mathcal{X}}_c(s\bar{n})(1 + \gamma_5) \frac{\not{h}}{2} \mathcal{X}_c(0) \bar{\mathcal{Q}}_{\bar{s}}(t\bar{n})(1 + \gamma_5) \frac{\not{h}}{2} \frac{n^\mu}{n \cdot v} \mathcal{H}_{\bar{s}}(0) \bar{\ell} \gamma_\mu \ell, \quad (30)$$

and obviously the corresponding jet function at tree level is trivial, $\mathcal{J}^C = 1$.

C. Matrix elements of SCET operators

The last step before we can finally get the decay amplitude of $B \rightarrow K^* \ell^+ \ell^-$ decay is to take the matrix elements of the relevant SCET operators. For A-type SCET currents, one may simply define [20]

$$\langle M(p) | \bar{\mathcal{X}}_{hc} \Gamma h | B(v) \rangle = -2E \zeta_M(E) \text{tr} [\bar{\mathcal{M}}_M(n) \Gamma \mathcal{M}_B(v)], \quad (31)$$

where the spinor wave functions are

$$\mathcal{M}_B(v) = -\frac{1 + \not{v}}{2} \gamma_5, \quad \bar{\mathcal{M}}_{K_\perp^*}(n) = \not{\varepsilon}_\perp^* \frac{\not{h} \not{h}}{4}, \quad \bar{\mathcal{M}}_{K_\parallel^*}(n) = -\frac{\not{h} \not{h}}{4}, \quad (32)$$

with ε the polarization vector of the K^* meson. It is then straightforward to get the matrix elements of the SCET_I currents J_i^A as

$$\begin{aligned} \langle K^* \ell^+ \ell^- | J_1^A | B \rangle &= -2E \zeta_\perp (g_\perp^{\mu\nu} - i\epsilon_\perp^{\mu\nu}) \varepsilon_{\perp\nu}^* \bar{\ell} \gamma_\mu \ell, & \langle K^* \ell^+ \ell^- | J_2^A | B \rangle &= -2E \zeta_\parallel \frac{n^\mu}{n \cdot v} \bar{\ell} \gamma_\mu \ell, \\ \langle K^* \ell^+ \ell^- | J_3^A | B \rangle &= -2E \zeta_\perp (g_\perp^{\mu\nu} - i\epsilon_\perp^{\mu\nu}) \varepsilon_{\perp\nu}^* \bar{\ell} \gamma_\mu \gamma_5 \ell, & \langle K^* \ell^+ \ell^- | J_4^A | B \rangle &= -2E \zeta_\parallel \frac{n^\mu}{n \cdot v} \bar{\ell} \gamma_\mu \gamma_5 \ell, \end{aligned} \quad (33)$$

where $g_{\perp}^{\mu\nu} \equiv g^{\mu\nu} - (n^{\mu}\bar{n}^{\nu} + \bar{n}^{\mu}n^{\nu})/2$ and $\epsilon_{\perp}^{\mu\nu} \equiv \epsilon^{\mu\nu\rho\sigma}v_{\rho}n_{\sigma}/(n \cdot v)$. Note that we use the convention $\epsilon^{0123} = +1$ in the above equations.

For B-type SCET_{II} operators, although naively the soft and collinear degrees of freedom seem to be decoupled, the factorization may be invalidated unless no endpoint divergences appear in the convolution integrals [27, 28]. The relevant meson LCDAs are defined as

$$\begin{aligned} \langle 0|\bar{Q}_s(tn)\Gamma\mathcal{H}_s(0)|B(v)\rangle &= \frac{iF(\mu)}{2}\sqrt{m_B}\int_0^{\infty}d\omega e^{-i\omega n\cdot vt} \\ &\quad \text{tr}\left[\left(\phi_+^B(\omega,\mu) - \frac{\not{n}}{2n\cdot v}(\phi_-^B(\omega,\mu) - \phi_+^B(\omega,\mu))\right)\Gamma\mathcal{M}_B(v)\right], \quad (34) \\ \langle K^*(p)|\bar{\mathcal{X}}_c(s\bar{n})\Gamma\frac{\not{n}}{2}\mathcal{X}_c(0)|0\rangle &= \frac{if_{K^*}(\mu)}{4}\bar{n}\cdot p\text{tr}[\overline{\mathcal{M}}_{K^*}\Gamma]\int_0^1du e^{ius\bar{n}\cdot p}\phi_{K^*}(u,\mu). \end{aligned}$$

With the above LCDAs, the matrix elements of the operators O_i^B can be written as

$$\begin{aligned} \langle K^*\ell^+\ell^-|C_1^BO_1^B|B\rangle &= -\frac{F(\mu)m_B^{3/2}}{4}(1-\hat{s})(g_{\perp}^{\mu\nu} - i\epsilon_{\perp}^{\mu\nu})\varepsilon_{\perp\nu}^*\bar{\ell}\gamma_{\mu}\ell\int_0^{\infty}\frac{d\omega}{\omega}\phi_+^B(\omega,\mu) \\ &\quad \times\int_0^1du f_{K_{\perp}^*}(\mu)\phi_{K_{\perp}^*}(u,\mu)\int_0^1dv\mathcal{J}_{\perp}(u,v,\ln\frac{m_b\omega(1-\hat{s})}{\mu^2},\mu)C_1^B(v,\mu) \\ &\equiv -\frac{F(\mu)m_B^{3/2}}{4}(1-\hat{s})(g_{\perp}^{\mu\nu} - i\epsilon_{\perp}^{\mu\nu})\varepsilon_{\perp\nu}^*\bar{\ell}\gamma_{\mu}\ell\phi_+^B\otimes f_{K_{\perp}^*}\phi_{K_{\perp}^*}\otimes\mathcal{J}_{\perp}\otimes C_1^B, \\ \langle K^*\ell^+\ell^-|C_2^BO_2^B|B\rangle &= -\frac{F(\mu)m_B^{3/2}}{4}(1-\hat{s})\frac{n^{\mu}}{n\cdot v}\bar{\ell}\gamma_{\mu}\ell\phi_+^B\otimes f_{K_{\parallel}^*}\phi_{K_{\parallel}^*}\otimes\mathcal{J}_{\parallel}\otimes C_2^B, \end{aligned} \quad (35)$$

while for the matrix element of $C_3^BO_3^B(C_4^BO_4^B)$, it can be obtained by simply replacing the lepton current $\bar{\ell}\gamma_{\mu}\ell$ on the right hand side of the above equations by $\bar{\ell}\gamma_{\mu}\gamma_5\ell$ and also replacing $C_1^B \rightarrow C_3^B$ ($C_2^B \rightarrow C_4^B$).

The matrix element of O^C is obtained likewise, with the result

$$\langle K^*\ell^+\ell^-|O^C|B\rangle = \frac{F(\mu)m_B^{3/2}}{4}(1-\hat{s})q^2\frac{n^{\mu}}{n\cdot v}\bar{\ell}\gamma_{\mu}\ell\frac{\omega\phi_-^B}{\omega - q^2/m_b - i\epsilon}\otimes f_{K_{\parallel}^*}\phi_{K_{\parallel}^*}\otimes\widehat{C}^C. \quad (36)$$

Since $\phi_-^B(\omega)$ does not vanish as ω approaches zero, the integral $\int d\omega\phi_-^B(\omega)/(\omega - q^2/m_b)$ would be divergent if $q^2 \rightarrow 0$. This endpoint singularity will violate the SCET_{II} factorization, that is why we should restrict our attention to the kinematic situation that the invariant mass of the lepton pair is not too small, say $q^2 \geq 1\text{ GeV}^2$.

D. Resummation of logarithms in SCET

In the above analysis a two-step matching process QCD \rightarrow SCET_I \rightarrow SCET_{II} has been implemented. This introduces two matching scales, $\mu_h \sim m_b$ at which QCD is matched

onto SCET_I and $\mu_l \sim \sqrt{m_b \Lambda}$ at which SCET_I is matched onto SCET_{II}. Thus, with the SCET_I matching coefficients at scale μ_h , one may use the renormalization-group equations (RGE) of SCET_I to evolve them down to scale μ_l and then match onto SCET_{II}. The large logarithms due to different scales are resummed during this process. Note that the meson LCDAs may be given at another scale μ_L , and, in principle, one should also use the RGE of SCET_{II} to run the corresponding matching coefficients from μ_l down to μ_L . But since in B decays the scale $\mu_l \simeq 1.5\text{GeV}$ is already quite low, we may just take the meson LCDAs at scale μ_l in this paper for simplicity and thereby avoid the running of the SCET_{II} matching coefficients.

Furthermore, one should note that for A-type SCET currents, only the scale μ_h is involved since it is not necessary to do the second step matching of SCET_I \rightarrow SCET_{II}. Therefore similarly, we may choose the nonperturbative form factor $\zeta_{\perp, \parallel}$ at scale μ_h and avoid the RGE running of A-type SCET_I matching coefficients. For B-type currents, the RGE of SCET_I can be obtained by calculating the anomalous dimensions of the relevant SCET operators, which has been done in [25], where the matching coefficients at any scale can be obtained by evolution from the matching scale μ_h

$$\begin{aligned} C_j^B(E, u, \mu) &= \left(\frac{2E}{\mu_h}\right)^{a(\mu_h, \mu)} e^{S(\mu_h, \mu)} \int_0^1 dv U_\Gamma(u, v, \mu_h, \mu) C_j^B(E, v, \mu_h) \\ &\equiv \left(\frac{2E}{\mu_h}\right)^{a(\mu_h, \mu)} e^{S(\mu_h, \mu)} \tilde{U}_\Gamma^j(E, u, \mu_h, \mu), \end{aligned} \quad (37)$$

with the subscript $\Gamma = \perp, \parallel$ and the functions $a(\mu_h, \mu)$ and $S(\mu_h, \mu)$ are given in Eq. (66) in Ref. [25]. Note that in the above equation one should use the subscript $\Gamma = \perp$ for $j = 1, 3$, while $\Gamma = \parallel$ for $j = 2, 4$. The evolution kernel $\tilde{U}_\Gamma^j(E, u, \mu_h, \mu)$ obeys

$$\frac{d\tilde{U}_\Gamma^j(E, u, \mu_h, \mu)}{d \ln \mu} = \int_0^1 dy y V_\Gamma(y, u) \tilde{U}_\Gamma^j(E, y, \mu_h, \mu) + \omega(u) \tilde{U}_\Gamma^j(E, u, \mu_h, \mu), \quad (38)$$

with the initial condition $\tilde{U}_\Gamma^j(E, u, \mu_h, \mu_h) = C_j^B(E, u, \mu_h)$. Again, the functions $V_\Gamma(y, u)$ and $\omega(u)$ are defined in [25]. In the next section of phenomenological application, we will solve the above integro-differential equation numerically.

Finally, for the C-type SCET current J^C , its anomalous dimension just equals the sum of the anomalous dimension of the K^* meson LCDA and that of the B meson LCDA ϕ_-^B . However since the evolution equation of ϕ_-^B is still unknown, we will not resum the perturbative logarithms for the J^C current in this paper. Numerically the contribution from

the J^C current to the decay amplitude is small. Furthermore, as we will see later, the J^C current is completely irrelevant for the forward-backward asymmetry of the charged lepton. Therefore, this treatment has only minor impact on our phenomenological discussion.

III. NUMERICAL ANALYSIS OF $B \rightarrow K^* \ell^+ \ell^-$

We are now in the position to write the decay amplitude of $B \rightarrow K^* \ell^+ \ell^-$, using the similar notations adopted in [14],

$$\begin{aligned} \frac{d^2\Gamma}{dq^2 d\cos\theta} &= \frac{G_F^2 |V_{ts}^* V_{tb}|^2}{128\pi^3} \left(\frac{\alpha_{em}}{4\pi}\right)^2 m_B^3 |\lambda_{K^*}| \left(1 - \frac{q^2}{m_B^2}\right)^2 \times \\ &\left\{ 2\zeta_{\perp}^2 (1 + \cos^2\theta) \frac{q^2}{m_B^2} (|\mathcal{C}_9^{\perp}|^2 + (\mathcal{C}_{10}^{\perp})^2) \right. \\ &\left. - 8\zeta_{\perp}^2 \cos\theta \frac{q^2}{m_B^2} \text{Re}(\mathcal{C}_9^{\perp}) \mathcal{C}_{10}^{\perp} + \zeta_{\parallel}^2 (1 - \cos^2\theta) (|\mathcal{C}_9^{\parallel}|^2 + (\mathcal{C}_{10}^{\parallel})^2) \right\}, \end{aligned} \quad (39)$$

with $m_B \lambda_{K^*}/2$ the momentum of the K^* meson in the rest frame of the B meson,

$$|\lambda_{K^*}| = \left[\left(1 - \frac{q^2}{m_B^2}\right)^2 - 2\frac{m_{K^*}^2}{m_B^2} \left(1 + \frac{q^2}{m_B^2}\right) + \frac{m_{K^*}^4}{m_B^4} \right]^{1/2}. \quad (40)$$

The angle θ denotes the angle between the momentum of the positively charged lepton and that of the B meson in the rest frame of the lepton pair. Notice that in the above equations the leptons are taken in the massless limit and the K^* meson mass is kept nonzero only for λ_{K^*} , which arises from the phase space. The "effective" Wilson coefficients $\mathcal{C}_9^{\perp,\parallel}$ and $\mathcal{C}_{10}^{\perp,\parallel}$ are given by

$$\begin{aligned} \mathcal{C}_9^{\perp} &= \frac{2\pi}{\alpha_{em}} \left(C_1^A + \frac{m_B}{4} \frac{f_B \phi_+^B \otimes f_{K^*}^{\perp} \phi_{K^*}^{\perp} \otimes \mathcal{J}_{\perp} \otimes C_1^B}{\zeta_{\perp}} \right), \\ \mathcal{C}_9^{\parallel} &= \frac{2\pi}{\alpha_{em}} \left(C_2^A + \frac{m_B}{4} \frac{f_B \phi_+^B \otimes f_{K^*}^{\parallel} \phi_{K^*}^{\parallel} \otimes \mathcal{J}_{\parallel} \otimes C_2^B}{\zeta_{\parallel}} \right. \\ &\quad \left. - \frac{q^2}{4m_B} \frac{f_B \omega \phi_-^B / (\omega - q^2/m_b) \otimes f_{K^*} \phi_{K^*} \otimes \widehat{C}^C}{\zeta_{\parallel}} \right), \\ \mathcal{C}_{10}^{\perp} &= \frac{2\pi}{\alpha_{em}} C_3^A, \\ \mathcal{C}_{10}^{\parallel} &= \frac{2\pi}{\alpha_{em}} \left(C_4^A + \frac{m_B}{4} \frac{f_B \phi_+^B \otimes f_{K^*}^{\parallel} \phi_{K^*}^{\parallel} \otimes \mathcal{J}_{\parallel} \otimes C_4^B}{\zeta_{\parallel}} \right), \end{aligned} \quad (41)$$

where $C_i^{A,B,C}$ are defined in Eq. (13). The above expressions are valid at leading power of $1/m_b$ and to all orders of α_s . But in this paper we only calculate explicitly the "effective

Wilson coefficients” at one-loop order. At this order our results are quite similar to those of [14] using the large-energy limit of QCD. The main phenomenological improvement is that for the hard scattering part, the matching coefficients C_i^B are evolved from the scale $\mu_h \sim \mathcal{O}(m_b)$ down to $\mu_l \sim \sqrt{m_b \Lambda_h}$, during which the perturbative logarithms are summed. Here Λ_h represents a typical hadronic scale. Note also that the definitions of the soft form factors $\zeta_{\perp, \parallel}$ in SCET are different from those of Ref [14], therefore the explicit expressions of C_i^A are also different from the coefficients $C_a^{0,1}$ appearing in [14] which are related to the form factor corrections.

In terms of the helicity amplitudes for the decay $B \rightarrow K^*(\rightarrow K + \pi)\ell^+\ell^-$, the double differential distribution $d^2\mathcal{B}/d\cos\theta_+ds$ is given in Eq.(44) of Ref. [29]. This requires the helicity amplitudes, $|H_0(s)|^2 = |H_0(s)^L|^2 + |H_0(s)^R|^2$, $|H_-^{L,R}(s)|^2$ and $|H_+^{L,R}(s)|^2$. While the amplitudes $H_+^{L,R}(s)$ are both power suppressed in $1/m_b$ and numerically small, the expressions for the others in SCET are given below:

$$\begin{aligned} |H_0|^2 &= \frac{m_B^2}{2} \left(1 - \frac{q^2}{m_B^2}\right)^2 (|\mathcal{C}_9^\parallel|^2 + (\mathcal{C}_{10}^\parallel)^2) \zeta_\parallel^2, \\ |H_-^{L,R}|^2 &= q^2 \left(1 - \frac{q^2}{m_B^2}\right)^2 |\mathcal{C}_9^\perp \pm \mathcal{C}_{10}^\perp|^2 \zeta_\perp^2. \end{aligned} \quad (42)$$

Note that the dependence on the soft form factors factorizes in ζ_\parallel^2 and ζ_\perp^2 for the helicity components $|H_0|^2$ and $|H_-^{L,R}|^2$, respectively. Since a similar analysis in terms of the helicity amplitudes of the charged current decay $B \rightarrow \rho(\pi\pi)\ell^+\nu_\ell$ can be performed, the ratios $R_0(s)$ and $R_-(s)$ of the two differential distributions (in $B \rightarrow K^*(\rightarrow K\pi)\ell^+\ell^-$ and $B \rightarrow \rho(\pi\pi)\ell^+\nu_\ell$) have lot less hadronic uncertainties, as these ratios (see Eq. (76) in Ref. [29] for their definition) involve estimates of SU(3)-breakings in the soft form factors. The point is that the ratios $\zeta_\parallel^{K^*}/\zeta_\parallel^\rho$ and $\zeta_\perp^{K^*}/\zeta_\perp^\rho$ are more reliably calculable than the form factors themselves.

A. Input parameters

To get the differential distributions numerically some input parameters have to be specified. For the calculation of the Wilson coefficients, the relevant parameters are chosen as [30]

$$M_W = 80.425 \text{ GeV}, \quad \sin^2 \theta_W = 0.2312, \quad \Lambda_{\overline{MS}}^{(5)} = 217_{-23}^{+25} \text{ MeV} \quad (43)$$

and $m_t^{pole} = (172.7 \pm 2.9) \text{ GeV}$, updated recently by the Tevatron electroweak group [31]. Numerical values of the Wilson coefficients, evaluated at scale $\mu = m_b = 4.8 \text{ GeV}$, with

three-loop running of α_s and the input parameters fixed at their central values given above are shown in Table I. Note that the NNLL formula for C_9 can be found, for example, in the appendix of [14], while the relevant elements of three-loop anomalous dimension matrix have been calculated recently in [32, 33].

TABLE I: The leading-logarithmic (LL) and next-to-leading-logarithmic (NLL) Wilson coefficients evaluated at the scale $m_b = 4.8$ GeV. For $C_{9,10}$, they are also given in NNLL order.

	LL	NLL		LL	NLL	NNLL
\bar{C}_1	-0.2501	-0.1459	\bar{C}_6	-0.0316	-0.0388	
\bar{C}_2	1.1082	1.0561	C_7^{eff}	-0.3145	-0.3054	
\bar{C}_3	0.0112	0.0116	C_8^{eff}	-0.1491	-0.1678	
\bar{C}_4	-0.0257	-0.0337	C_9	1.9919	4.1777	4.2120
\bar{C}_5	0.0075	0.0097	C_{10}	0	-4.5415	-4.1958

The CKM factor $|V_{ts}V_{tb}^*| \simeq (1 - \lambda^2/2)|V_{cb}|$ is estimated to be 0.0403 ± 0.0020 by taking $|V_{cb}| = 0.0413 \pm 0.0021$ [34] and $\lambda = 0.2226$. For the B meson lifetime, we use $\tau_{B^+} = 1.643$ ps, $\tau_{B^0} = 1.528$ ps [34]. The pole mass m_b is chosen to be 4.8 GeV. The ratio of charm quark mass over b-quark mass is taken to be $m_c/m_b = 0.29 \pm 0.02$. For the matching scale from SCET_I to SCET_{II}, we use $\mu_l = \sqrt{m_b \Lambda_h} \simeq 1.5$ GeV.

The hadronic parameters for the decay $B \rightarrow K^* \ell^+ \ell^-$ include decay constants, light-cone distribution amplitudes (LCDAs) and the soft form factors. The B meson decay constant can be estimated by QCD sum rules or lattice calculations, here we take $f_B = (200 \pm 30)$ MeV. For the K^* meson, experimental measurements give [30] $f_{K^*}^{\parallel} = (217 \pm 5)$ MeV while the most recent light-cone sum rules (LCSRs) estimate [35] $f_{K^*}^{\perp}(1 \text{ GeV}) = (185 \pm 10)$ MeV. Notice that $f_{K^*}^{\perp}$ obeys the scale evolution equation $f_{K^*}^{\perp}(\mu) = f_{K^*}^{\perp}(\mu_0)(\alpha_s(\mu)/\alpha_s(\mu_0))^{4/23}$.

The B meson LCDAs enter into the decay amplitudes only in terms of the integrated quantities $\lambda_{B,+}^{-1}$ and $\lambda_{B,-}^{-1}(q^2)$ defined as by the following integrals

$$\lambda_{B,+}^{-1} \equiv \int_0^{\infty} \frac{d\omega}{\omega} \phi_+^B(\omega), \quad \lambda_{B,-}^{-1}(q^2) \equiv \int_0^{\infty} d\omega \frac{\phi_-^B(\omega)}{\omega - q^2/m_b - i\epsilon}. \quad (44)$$

Therefore, it is not necessary to know the details about the shape of $\phi_+^B(\omega)$. The most recent estimate gives [36] $\lambda_{B,+}^{-1} = (1.86 \pm 0.34) \text{ GeV}^{-1}$ at the scale $\mu = 1.5$ GeV. However, $\lambda_{B,-}^{-1}(q^2)$

does require the knowledge of $\phi_-^B(\omega)$, about which we know very little. Fortunately, $\lambda_{B,-}^{-1}(q^2)$ only appears in the annihilation term which plays numerically a minor role in $B \rightarrow K^* \ell^+ \ell^-$ decay. To be definite, we adopt a simple model function [37] $\phi_-^B(\omega) = \omega_0^{-1} e^{-\omega/\omega_0}$ with $\omega_0^{-1} \simeq 3 \text{ GeV}^{-1}$.

The K^* meson LCDA may be expanded in terms of Gegenbauer polynomials:

$$\phi_{K^*}^{\perp,\parallel}(u, \mu) = 6u(1-u) \left[1 + \sum_{n=1}^{\infty} a_n^{\perp,\parallel}(\mu) C_n^{3/2}(2u-1) \right]. \quad (45)$$

However, the coefficients a_n are largely unknown. Following [38], we shall ignore the terms $a_n^{\perp,\parallel}$ ($n > 2$). For $a_{1,2}$, we omit their scale dependences and estimate in a conservative manner: $a_1^{\perp,\parallel} = 0.1 \pm 0.1$, $a_2^{\perp,\parallel} = 0.1 \pm 0.1$. We note that recently the first Gegenbauer moment of the K^* meson has been revisited in LCSRs [35] which gives smaller uncertainties.

There are only two independent $B \rightarrow K^*$ form factors in SCET, namely $\zeta_{\perp}(q^2)$ and $\zeta_{\parallel}(q^2)$. They are related to the full QCD form factors as discussed in [25]. The current knowledge of these form factors is fragmentary. For instance, ζ_{\perp} may be extracted from $V^{B \rightarrow K^*}$ [20]:

$$\zeta_{\perp}(q^2) = \frac{\zeta_{\perp}(0)}{r_1^V + r_2^V} \left(\frac{r_1^V}{1 - q^2/m_V^2} + \frac{r_2^V}{1 - q^2/m_{V_{fit}}^2} \right), \quad (46)$$

with $r_1^V = 0.923$, $r_2^V = -0.511$, $m_V = 5.32 \text{ GeV}$ and $m_{V_{fit}}^2 = 49.40 \text{ GeV}^2$. Note that the q^2 dependence above is the same as that of $V^{B \rightarrow K^*}(q^2)$, calculated in [38] using LCSRs. However, analyses of the radiative B decays $B \rightarrow K^* \gamma$ [14, 20, 39, 40], $B \rightarrow \rho \gamma$ [39, 40] and the semi-leptonic B decay $B \rightarrow \rho \ell \nu$ [41] imply that the LCSRs overestimate the $B \rightarrow V$ form factors significantly. We use the radiative $B \rightarrow K^* \gamma$ decay, which has been measured quite precisely [34]: $\mathcal{B}(B^0 \rightarrow K^{*0} \gamma) = (4.01 \pm 0.20) \times 10^{-5}$, to normalize the soft form factor at $q^2 = 0$. In SCET, it is straight forward to get the decay amplitude of $B \rightarrow K^* \gamma$ from the $B \rightarrow K^* \ell^+ \ell^-$ decay, by taking the limit $q^2 \rightarrow 0$. Then, using the input parameters from Table II, we obtain $\zeta_{\perp}(0) = 0.32 \pm 0.02$. Here the error is mainly from the CKM factor $V_{ts} V_{tb}^*$ and the experimental uncertainty of the branching ratio $\mathcal{B}(B^0 \rightarrow K^{*0} \gamma)$. This estimate is consistent with the result of Ref. [20], but significantly smaller than the number 0.40 ± 0.04 we get from LCSRs. In our numerical analysis, we will choose the value $\zeta_{\perp}(0) = 0.32 \pm 0.02$ determined from the radiative B decays, but assume that the q^2 -dependence of $\zeta_{\perp}(q^2)$ can be reliably obtained from the LCSRs.

For the longitudinal soft form factor ζ_{\parallel} , unfortunately there is no quantitative determination from the existing experiments, though this may change in the future with good quality

TABLE II: Numerical values of the input parameters and their uncertainties used in the phenomenological study.

M_W	80.425 GeV	$\sin^2 \theta_W$	0.2312
m_t^{pole}	(172.7 ± 2.9) GeV	$\Lambda_{\overline{MS}}^{(5)}$	(217_{-23}^{+25}) MeV
$ V_{ts}V_{tb}^* $	$(40.3 \pm 2.0) \times 10^{-3}$	$\alpha_{em}(m_b)$	1/133
m_B	5.279 GeV	m_b^{pole}	4.8 GeV
τ_{B^+}	1.643 ps	τ_{B^0}	1.528 ps
m_c/m_b	0.29 ± 0.02	μ_l	1.5 GeV
$\lambda_{B,+}^{-1}(1.5 \text{ GeV})$	(1.86 ± 0.34) GeV $^{-1}$	f_B	(200 ± 30) MeV
$\zeta_{\perp}(0)$	0.32 ± 0.02	$\zeta_{\parallel}(0)$	0.40 ± 0.05
$f_{K^*}^{\perp}(1 \text{ GeV})$	(185 ± 10) MeV	$f_{K^*}^{\parallel}$	(217 ± 5) MeV
$a_1^{\perp,\parallel}$	0.1 ± 0.1	$a_2^{\perp,\parallel}$	0.1 ± 0.1

data available on the decay $B \rightarrow \rho \ell \nu_{\ell}$. Using helicity analysis, one can extract $\zeta_{\parallel}^{\rho}(q^2)$; combined with estimates of the SU(3)-breaking one may determine $\zeta_{\parallel}^{K^*}(q^2)$. Not having this experimental information at hand, one may extract $\zeta_{\parallel}(q^2)$ from the full QCD form factor $A_0^{B \rightarrow K^*}(q^2)$:

$$A_0^{B \rightarrow K^*}(q^2) = \left[1 - \frac{\alpha_s(m_b)C_F}{4\pi} \left(2 \ln^2[1-s] - \frac{2}{s} \ln[1-s] + 2 Li_2[s] + 4 + \frac{\pi^2}{12} \right) \right] \zeta_{\parallel} - \frac{1}{4(1-s)} f_B \phi_+^B \otimes f_{K^*}^{\parallel} \phi_{K^*}^{\parallel} \otimes \mathcal{J}_{\parallel} \otimes \left(\frac{2E}{\mu_h} \right)^{a(\mu_h, \mu_l)} e^{S(\mu_h, \mu_l)} \int_0^1 dy U_{\parallel}(v, y, \mu_h, \mu_l) \quad (47)$$

with $s = q^2/m_B^2$. LCSRs estimate [38] $A_0(0) = 0.374 \pm 0.043$ with the q^2 -dependence

$$A_0(q^2) = \frac{1.364}{1 - q^2/m_B^2} - \frac{0.990}{1 - q^2/36.78 \text{GeV}^2} . \quad (48)$$

From which we get $\zeta_{\parallel}(0) = 0.40 \pm 0.05$, using the input parameters discussed above and/or listed in Table II. Its q^2 -dependence is drawn in Fig. 4.

Alternatively, ζ_{\parallel} may also be determined from the following relation,

$$\frac{Em_B(V - A_2)}{m_{K^*}(m_B + m_{K^*})} = \left[1 - \frac{\alpha_s(m_b)C_F}{4\pi} \left(2 \ln^2[1-s] - 2 \ln[1-s] + 2 Li_2[s] + 6 + \frac{\pi^2}{12} \right) \right] \zeta_{\parallel} - \frac{1-2s}{4(1-s)} f_B \phi_+^B \otimes f_{K^*}^{\parallel} \phi_{K^*}^{\parallel} \otimes \mathcal{J}_{\parallel} \otimes \left(\frac{2E}{\mu_h} \right)^{a(\mu_h, \mu_l)} e^{S(\mu_h, \mu_l)} \int_0^1 dy U_{\parallel}(v, y, \mu_h, \mu_l) . \quad (49)$$

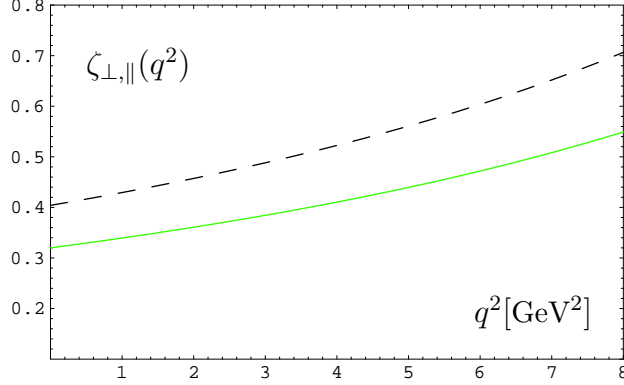


FIG. 4: The q^2 -dependence of the soft form factors $\zeta_{\perp,\parallel}(q^2)$. The solid curve represents $\zeta_{\perp}(q^2)$, while the dashed curve represents $\zeta_{\parallel}(q^2)$. We have rescaled the transverse form factor at $q^2 = 0$, to be consistent with the experimental measurements of the $B \rightarrow K^* \gamma$ decay rate.

With the input $V^{B \rightarrow K^*}(0) - A_2^{B \rightarrow K^*}(0) = 0.152 \pm 0.057$ from LCSRs, we obtain $\zeta_{\parallel}(0) = 0.42 \pm 0.16$, which agrees with the range extracted from $A_0^{B \rightarrow K^*}$. We will use $\zeta_{\parallel}(0) = 0.40 \pm 0.05$, obtained from its relation to the full form factor $A_0^{B \rightarrow K^*}$ and the LCSR, as discussed above. Fig. 4 shows the q^2 -dependence of both soft form factors $\zeta_{\perp,\parallel}(q^2)$. However, since the analysis of the semileptonic decay $B \rightarrow \rho \ell \nu$ [41] suggests that both the transverse and longitudinal form factors might be overestimated by LCSRs, we will also consider, as an illustration of the non-perturbative uncertainties, the value $\zeta_{\parallel}(0) = \zeta_{\perp}(0) = 0.32$ with all the other parameters taken at their central values.

B. Numerical solution of the SCET_I evolution functions

As we discussed in Sect. II.D, the B-type matching coefficients C_i^B should be run from the scale $\mu_h = 4.8$ GeV down to $\mu_l = 1.5$ GeV, with the evolution kernel $\tilde{U}_{\Gamma}(E, u, \mu_h, \mu)$ obeying the integro-differential equation (38). To solve this equation numerically, it is more convenient to define the following evolution functions,

$$\begin{aligned}
 \tilde{U}_{\Gamma}^{(a)}(E, u, \mu_h, \mu) &= \int_0^1 dv U_{\Gamma}(u, v, \mu_h, \mu) , \\
 \tilde{U}_{\Gamma}^{(b)}(E, u, \mu_h, \mu) &= \frac{u + \hat{s} - u\hat{s}}{1 - u} \int_0^1 dv U_{\Gamma}(u, v, \mu_h, \mu) \frac{1 - v}{v + \hat{s} - v\hat{s}} , \\
 \tilde{U}_{\Gamma}^{(c)}(E, u, \mu_h, \mu) &= \int_0^1 dv U_{\Gamma}(u, v, \mu_h, \mu) \frac{F_{16}^{\Gamma}(v, \hat{s}, m_c^2/m_b^2)}{F_{16}^{\Gamma}(u, \hat{s}, m_c^2/m_b^2)} ,
 \end{aligned} \tag{50}$$

where $\Gamma = \perp, \parallel$ and the functions $F_{16}^{\perp, \parallel}(u, \hat{s}, m_c^2/m_b^2)$ are defined in Eqs. (18) and (19). Notice that at quark level, the K^* meson energy is related to \hat{s} by $E = m_b(1 - \hat{s})/2$. With such definitions, the above evolution functions are normalized to one at the scale μ_h : $\tilde{U}_\Gamma^{(a,b,c)}(E, u, \mu_h, \mu_h) = 1$, and the QCD parameter $\Lambda_{\overline{MS}}^{(5)}$ would be the only input for their numerical evaluations. The matching coefficients C_j^B at scale μ_l can then be written as

$$\Delta_i C_j^B(E, u, \mu_l) = \left(\frac{2E}{\mu_h}\right)^{a(\mu_h, \mu_l)} e^{S(\mu_h, \mu_l)} \tilde{U}_\Gamma^{(a,b,c)}(E, u, \mu_h, \mu_l) \Delta_i C_j^B(E, u, \mu_h), \quad (51)$$

where we should use the superscript (a) for $\Delta_{7,9,10} C_j^B$, the superscript (b) for $\Delta_8 C_j^B$ and the superscript (c) for $\Delta_{16} C_j^B$. For the subscript Γ , one should use $\Gamma = \perp$ for $j = 1, 3$ and $\Gamma = \parallel$ for $j = 2, 4$, which is the same as the convention of Eq. (37). Notice that for the evolution of $\Delta_{16} C_j^B$, we have taken into account the fact that the term $F_{16}^\Gamma(u, \hat{s}, m_c^2/m_b^2)$ is dominant due to the large Wilson coefficient \bar{C}_2 .

It is then straightforward to get the following evolution equations

$$\begin{aligned} \frac{d\tilde{U}_\Gamma^{(a)}(E, u, \mu_h, \mu)}{d \ln \mu} &= \int_0^1 dy y V_\Gamma(y, u) \tilde{U}_\Gamma^{(a)}(E, y, \mu_h, \mu) + \omega(u) \tilde{U}_\Gamma^{(a)}(E, u, \mu_h, \mu), \\ \frac{d\tilde{U}_\Gamma^{(b)}(E, u, \mu_h, \mu)}{d \ln \mu} &= \int_0^1 dy y V_\Gamma(y, u) \frac{(1-y)(u + (1-u)\hat{s})}{(1-u)(y + (1-y)\hat{s})} \tilde{U}_\Gamma^{(b)}(E, y, \mu_h, \mu) + \\ &\quad \omega(u) \tilde{U}_\Gamma^{(b)}(E, u, \mu_h, \mu), \\ \frac{d\tilde{U}_\Gamma^{(c)}(E, u, \mu_h, \mu)}{d \ln \mu} &= \int_0^1 dy y V_\Gamma(y, u) \frac{F_{16}^\Gamma(y, \hat{s}, m_c^2/m_b^2)}{F_{16}^\Gamma(u, \hat{s}, m_c^2/m_b^2)} \tilde{U}_\Gamma^{(c)}(E, y, \mu_h, \mu) + \\ &\quad \omega(u) \tilde{U}_\Gamma^{(c)}(E, u, \mu_h, \mu). \end{aligned} \quad (52)$$

To get the numerical solutions of the above integro-differential equations, we will perform the scale evolution in one hundred discrete steps. While from the scale μ_n to μ_{n+1} , the convolution integral is evaluated for three hundred different values and discrete \hat{s} values of $\delta\hat{s} = 0.01$ in the interval $\hat{s} \in [0.04, 0.35]$. The function $\tilde{U}_\Gamma(E, u, \mu_h, \mu_{n+1})$ is obtained from a fit to these values. Taking $\Lambda_{\overline{MS}}^{(5)} = 217$ MeV, the numerical results of these evolution functions are shown in Fig. 5. Notice that, the function $\tilde{U}_\Gamma^{(a)}(E, u, \mu_h, \mu)$ shown in Fig. (5a) is actually the same as $U_\Gamma(u, \mu_h, \mu)$ defined in Eq. (5.23) of Neubert *et al.* [25]. The function $\tilde{U}_\parallel^{(b)}$ is not shown in Fig. 5, since it does not enter into the decay amplitude at one-loop level, due to $\Delta_8 C_2^B = 0$. While for the complex functions $\tilde{U}_\Gamma^{(c)}$, only the absolute values of the functions are plotted.

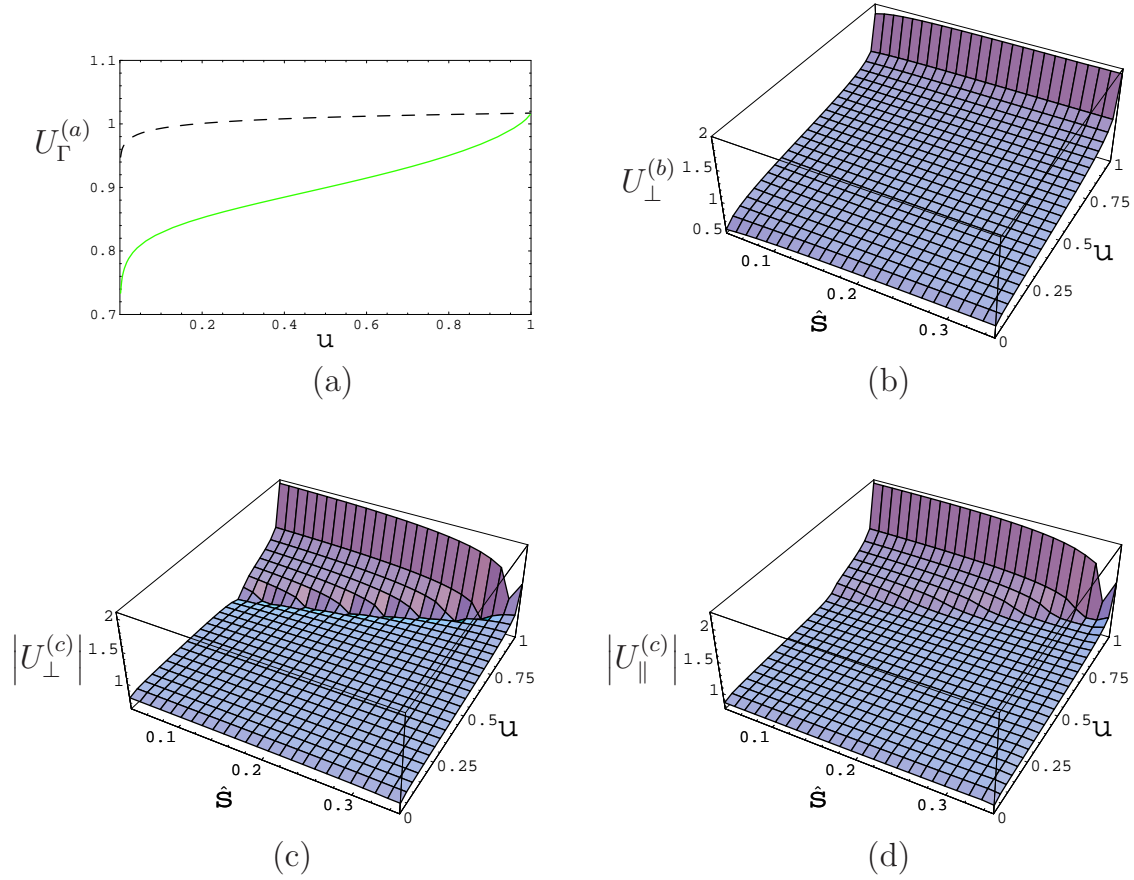


FIG. 5: Numerical values of the functions $\tilde{U}_\Gamma^{(a,b,c)}(E, u, \mu_h, \mu_l)$, evolved from $\mu_h = 4.8$ GeV down to $\mu_l = 1.5$ GeV. For the upper-left plot, the solid line denotes $\tilde{U}_\perp^{(a)}$ while the dashed line denotes $\tilde{U}_\parallel^{(a)}$. For the lower plots, since $\tilde{U}_\Gamma^{(c)}$ are complex functions, we only show their absolute values.

C. The dilepton invariant mass spectrum and the forward-backward asymmetry

Experimentally, the dilepton invariant mass spectrum and the forward-backward asymmetry are the observables of principal interest. Their theoretical expressions in SCET can be easily derived from Eq. (39):

$$\frac{dBr}{dq^2} = \tau_B \frac{G_F^2 |V_{ts}^* V_{tb}|^2}{128\pi^3} \left(\frac{\alpha_{em}}{4\pi}\right)^2 m_B^3 |\lambda_{K^*}| \left(1 - \frac{q^2}{m_B^2}\right)^2 \times \left\{ \frac{16}{3} \zeta_\perp^2 \frac{q^2}{m_B^2} (|\mathcal{C}_9^\perp|^2 + (\mathcal{C}_{10}^\perp)^2) + \frac{4}{3} \zeta_\parallel^2 (|\mathcal{C}_9^\parallel|^2 + (\mathcal{C}_{10}^\parallel)^2) \right\}, \quad (53)$$

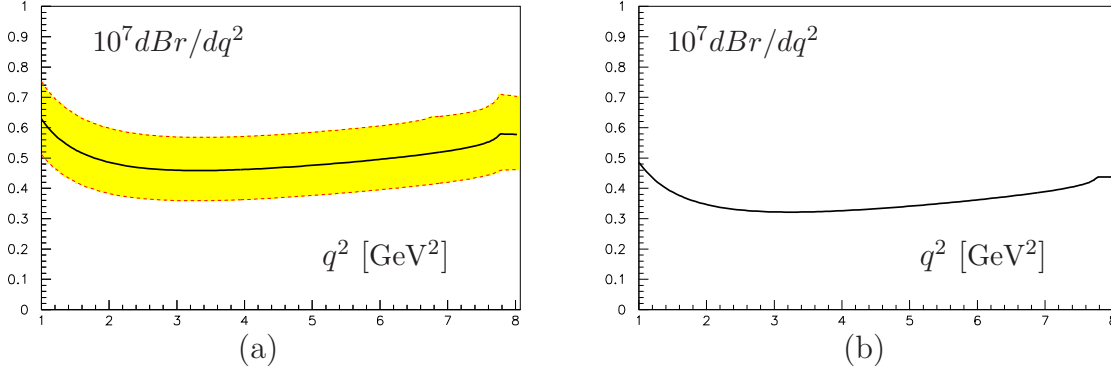


FIG. 6: The differential branching ratio $d\mathcal{B}(B^+ \rightarrow K^{*0}\ell^+\ell^-)/dq^2$ in the range $1 \text{ GeV}^2 \leq q^2 \leq 8 \text{ GeV}^2$. In the left plot, the solid line denotes the theoretical prediction with the input parameters taken at their central values, while the gray area between two dashed lines reflects the uncertainties from input parameters and scale dependence. In the right plot, the soft form factors are normalized as $\zeta_{\parallel}(0) = \zeta_{\perp}(0) = 0.32$, while all the other parameters are chosen at their central values.

$$\begin{aligned} \frac{dA_{FB}}{dq^2} &= \frac{1}{d\Gamma/dq^2} \left(\int_0^1 d\cos\theta \frac{d^2\Gamma}{dq^2 d\cos\theta} - \int_{-1}^0 d\cos\theta \frac{d^2\Gamma}{dq^2 d\cos\theta} \right) \\ &= \frac{-6(q^2/m_B^2)\zeta_{\perp}^2 \text{Re}(\mathcal{C}_9^{\perp})\mathcal{C}_{10}^{\perp}}{4(q^2/m_B^2)\zeta_{\perp}^2 (|\mathcal{C}_9^{\perp}|^2 + (\mathcal{C}_{10}^{\perp})^2) + \zeta_{\parallel}^2 (|\mathcal{C}_9^{\parallel}|^2 + (\mathcal{C}_{10}^{\parallel})^2)}. \end{aligned} \quad (54)$$

With the input parameters listed in Table II, The decay spectrum and the FB asymmetry are shown in Fig. 6 and Fig. 7, respectively. In our calculation we have dropped the small isospin-breaking effects, which come from the annihilation topology, and take the spectator quark as down quark in Eqs. (22, 23). To estimate the residual scale dependence, we vary the QCD matching scale μ_h by a factor $\sqrt{2}$ around the default value $\mu_h = m_b$. Notice that the soft form factors $\zeta_{\perp, \parallel}(q^2)$ defined in SCET are actually scale dependent, which effect has been taken into account in our error analysis.

Restricting to the integrated branching ratio of $B \rightarrow K^*\ell^+\ell^-$ in the range $1 \text{ GeV}^2 \leq q^2 \leq 7 \text{ GeV}^2$, where the SCET method should work, we obtain

$$\int_{1 \text{ GeV}^2}^{7 \text{ GeV}^2} dq^2 \frac{dBr(B^+ \rightarrow K^{*0}\ell^+\ell^-)}{dq^2} = (2.92_{-0.50}^{+0.57}|_{\zeta_{\parallel}} \text{ }_{-0.28}^{+0.30}|_{\text{CKM}} \text{ }_{-0.20}^{+0.18}) \times 10^{-7}. \quad (55)$$

Here we have isolated the uncertainties from the soft form factor ζ_{\parallel} and the CKM factor $|V_{ts}^*V_{tb}|$. The last error reflects the uncertainty due to the variation of the other input

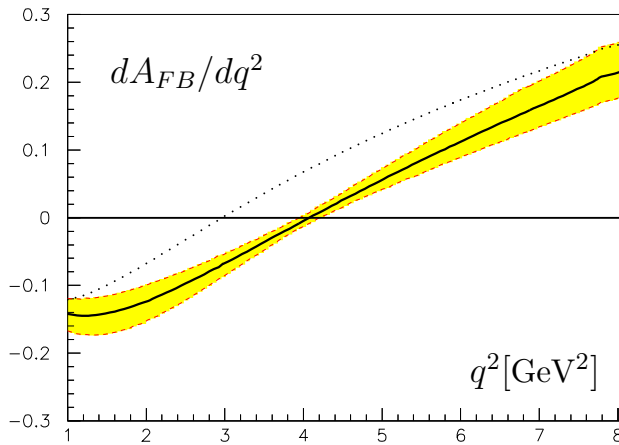


FIG. 7: The differential spectrum of the forward backward asymmetry $dA_{FB}(B \rightarrow K^*\ell^+\ell^-)/dq^2$ in the range $1 \text{ GeV}^2 \leq q^2 \leq 8 \text{ GeV}^2$. Here the solid line denotes the theoretical prediction with the input parameters taken at their central values, while the gray band between two dashed lines reflects the uncertainties from input parameters and scale dependence. The dotted line represents the LO predictions, obtained by dropping the $O(\alpha_s)$ corrections.

parameters and the residual scale dependence. If the smaller value for the longitudinal form factor $\zeta_{\parallel}(0) = 0.32$ is used, as shown in Fig. (6b), the central value of the branching ratio is reduced to 2.11×10^{-7} . For B^0 decay, the branching ratio is about 7% lower due to the lifetime difference:

$$\int_{1 \text{ GeV}^2}^{7 \text{ GeV}^2} dq^2 \frac{dBr(B^0 \rightarrow K^{*+}\ell^+\ell^-)}{dq^2} = (2.72_{-0.47}^{+0.53}|_{\zeta_{\parallel}} \text{ }_{-0.26}^{+0.28}|_{\text{CKM}} \text{ }_{-0.19}^{+0.17}) \times 10^{-7}. \quad (56)$$

To compare with the current experimental observations, it was proposed in Ref. [14] to consider the integrated branching ratio over the range $4 \text{ GeV}^2 \leq q^2 \leq 6 \text{ GeV}^2$, for which we get $(0.92_{-0.19}^{+0.21}) \times 10^{-7}$. This is smaller than the number $(1.2 \pm 0.4) \times 10^{-7}$ obtained in Ref. [14], which is mainly due to the fact that the most recent LCSR's estimation [38] prefers the form factor $A_0^{B \rightarrow K^*}$ to be smaller. Experimentally one of the Belle observations [4] of our interest is

$$\int_{4 \text{ GeV}^2}^{8 \text{ GeV}^2} dq^2 \frac{dBr(B \rightarrow K^*\ell^+\ell^-)}{dq^2} = (4.8_{-1.2}^{+1.4}|_{\text{stat.}} \pm 0.3|_{\text{syst.}} \pm 0.3|_{\text{model}}) \times 10^{-7}. \quad (57)$$

for which we predict $(1.94_{-0.40}^{+0.44}) \times 10^{-7}$. This is smaller than the published Belle data by a factor of about 2.5. But at this stage, it is still too early to conclude that one should change some theoretical input significantly to be consistent with the experimental data.

For instance, the BaBar collaboration measure the total branching ratio of $B \rightarrow K^* \ell^+ \ell^-$ to be [3] $(7.8_{-1.7}^{+1.9} \pm 1.2) \times 10^{-7}$, which is about twice smaller than the Belle observation [4] $(16.5_{-2.2}^{+2.3} \pm 0.9 \pm 0.4) \times 10^{-7}$. This implies that, if finally the total branching ratio of $B \rightarrow K^* \ell^+ \ell^-$ is found to be closer to the BaBar result, the partially integrated branching ratio over the range $4 \text{ GeV}^2 \leq q^2 \leq 8 \text{ GeV}^2$ could be lowered to around 2.3×10^{-7} , which is consistent with our estimate $(1.94_{-0.40}^{+0.44}) \times 10^{-7}$ within the stated errors. We look forward to experimental analyses from BABAR and BELLE based on their high statistic data.

One of the most interesting observables in the decay $B \rightarrow K^* \ell^+ \ell^-$ is the location, q_0^2 , where the FB asymmetry vanishes. It was first noticed in the context of form factor models in [42] and later demonstrated in [12], using the symmetries of the effective theory in the large-energy limit, that the value of q_0 is almost free of hadronic uncertainties at leading order. From Eq. (54), it is easy to see that the location of the vanishing FB asymmetry is determined by $Re(\mathcal{C}_9^\perp) = 0$. At the leading order, this leads to the equation $C_9 + C_7^{eff} + Re(Y(q_0^2)) = 0$. Including the order α_s corrections, our analysis estimates the zero-point of the FB asymmetry to be

$$q_0^2 = (4.07_{-0.12}^{+0.13}) \text{ GeV}^2 . \quad (58)$$

The corresponding range for q_0^2 from Beneke et al. [14] is: $q_0^2 = 4.2 \pm 0.6 \text{ GeV}^2$. While the central values are similar, the parameteric uncertainties are lot less in our estimate, as the residual scale dependence now contributes little to the uncertainties. Moreover, we have constrained the form factor $\zeta_\perp(q^2)$ from data on $B \rightarrow K^* \gamma$, and as the q^2 -range of interest does not require large extrapolation from the normalization point $q^2 = 0$, the residual error in $\zeta_\perp(q_0^2)$ is small. The uncertainty in $\zeta_\parallel(q^2)$, which is currently the dominant source of theoretical error, does not effect the zero-point q_0^2 , which follows from the first of Eqs. (41) showing that \mathcal{C}_9^\perp depends only on the form factor $\zeta_\perp(q^2)$. However, one should bear in mind that our error estimates only reflect the uncertainties from the input parameters to leading order in $1/m_b$. Power corrections in $1/m_b$ have not been considered here, although they are probably comparable to the $O(\alpha_s)$ corrections.

IV. SUMMARY

In this paper, we have examined the rare B decay channel $B \rightarrow K^* \ell^+ \ell^-$ in the framework of SCET, where the factorization formula holds to all orders in α_s and leading order in $1/m_b$.

Making use of the existing literature, we work with the relevant effective operators in SCET and the corresponding matching procedures are discussed in detail. The logarithms related to the different scales $\mu_h = m_b$ and $\mu_l = \sqrt{m_b \Lambda_h}$ are resummed by solving numerically the renormalization group equation in SCET. We then give explicit expressions for the differential distributions in q^2 for the decay $B \rightarrow K^* \ell^+ \ell^-$ including the $O(\alpha_s)$ corrections. In the phenomenological analysis, we first discuss the input parameters, especially how to extract the soft form factors $\zeta_{\perp, \parallel}(q^2)$ from the full QCD form factors and also the constraints on $\zeta_{\perp}(0)$ from the experimental data on the $B \rightarrow K^* \gamma$ decay. Using the q^2 -dependence of the form factors from the LCSRs and the normalization $\zeta_{\perp}(0) = 0.32 \pm 0.02$; $\zeta_{\parallel}(0) = 0.40 \pm 0.05$, we work out the differential branching ratio and the forward backward asymmetry as a function of the dilepton invariant mass. In the region $1 \text{ GeV}^2 \leq q^2 \leq 7 \text{ GeV}^2$, where the perturbative method should be reliable, our analysis yields

$$\int_{1 \text{ GeV}^2}^{7 \text{ GeV}^2} dq^2 \frac{dBr(B^+ \rightarrow K^{*0} \ell^+ \ell^-)}{dq^2} = (2.92_{-0.61}^{+0.67}) \times 10^{-7}, \quad (59)$$

which can be compared with the B factory measurements in the near future. The largest uncertainty in the branching ratio is due to the imprecise knowledge of $\zeta_{\parallel}(q^2)$. We have illustrated this by using a value $\zeta_{\parallel}(0) = 0.32$, which reduces the central value of the branching ratio to 2.11×10^{-7} . We point out that precisely measured q^2 -distributions in $B \rightarrow K^* \ell^+ \ell^-$ and $B \rightarrow \rho \ell \nu_{\ell}$ would greatly reduce the form-factor related uncertainties in the differential branching ratios. The FBA is less dependent on the soft form factors, and the residual parameteric dependencies are worked out. We estimate the zero-point of the FBA to be $q_0^2 = (4.07_{-0.12}^{+0.13}) \text{ GeV}^2$.

Acknowledgement

G.Z acknowledges the financial support from Alexander-von-Humboldt Stiftung. G.Z is also grateful to D.s. Yang for useful discussions.

-
- [1] J. Kaneko *et al.* [Belle Collaboration], Phys. Rev. Lett. **90**, 021801 (2003) [hep-ex/0208029].
 - [2] B. Aubert *et al.* [BABAR Collaboration], Phys. Rev. Lett. **93**, 081802 (2004) [hep-ex/0404006].

- [3] B. Aubert *et al.* [BaBar Collaboration], hep-ex/0507005, contributed to 22nd International Symposium on Lepton-Photon Interactions at High Energy (LP 2005), Uppsala, Sweden, 30 June - 5 July 2005.
- [4] K. Abe *et al.* [Belle Collaboration], hep-ex/0410006, presented at 32nd International Conference on High-Energy Physics (ICHEP 04), Beijing, China, 16-22 Aug 2004.
- [5] K. Abe *et al.* [Belle Collaboration], hep-ex/0508009.
- [6] A. Ali, T. Mannel and T. Morozumi, Phys. Lett. B **273**, 505 (1991).
- [7] N.G. Deshpande, J. Trampetic and K. Panose, Phys. Rev. D **39**, 1461 (1989).
- [8] C.S. Lim, T. Morozumi and A.I. Sanda, Phys. Lett. B **218**, 343 (1989).
- [9] A. Ali and T. Mannel, Phys. Lett. B **264**, 447 (1991); **274**, 526(E) (1992).
- [10] C. Greub, A. Ioannisian and D. Wyler, Phys. Lett. B **346**, 149 (1994).
- [11] D. Melikhov, N. Nikitin and S. Simula, Phys. Lett. B **410**, 290 (1997).
- [12] A. Ali, P. Ball, L.T. Handoko and G. Hiller, Phys. Rev. D **61**, 074024 (2000).
- [13] M. Beneke, G. Buchalla, M. Neubert and C.T. Sachrajda, Phys. Rev. Lett. **83**, 1914 (1999); Nucl. Phys. B **591**, 313 (2000).
- [14] M. Beneke, Th. Feldmann and D. Seidel, Nucl. Phys. B **612**, 25 (2001); Eur. Phys. J. C **41**, 173 (2005).
- [15] C.W. Bauer, S. Fleming and M.E. Luke, Phys. Rev. D **63**, 014006 (2001).
- [16] C.W. Bauer, S. Fleming, D. Pirjol and I.W. Stewart, Phys. Rev. D **63**, 114020 (2001).
- [17] C.W. Bauer and I. W. Stewart, Phys. Lett. B **516**, 134 (2001).
- [18] M. Beneke, A.P. Chapovsky, M. Diehl and Th. Feldmann, Nucl. Phys. B **643**, 431 (2002).
- [19] R.J. Hill and M. Neubert, Nucl. Phys. B **657**, 229 (2003).
- [20] T. Becher, R. J. Hill and M. Neubert, Phys. Rev. D **72**, 094017 (2005).
- [21] J.g. Chay and C. Kim, Phys. Rev. D **68**, 034013 (2003).
- [22] F. Krüger and L.M. Sehgal, Phys. Lett. B **380**, 199 (1996).
- [23] K. Chetyrkin, M. Misiak and M. Münz, Phys. Lett. B **400**, 206 (1997).
- [24] M. Beneke, Y. Kiyo and D. s. Yang, Nucl. Phys. B **692**, 232 (2004).
- [25] R.J. Hill, T. Becher, S.J. Lee and M. Neubert, JHEP **0407**, 081 (2004).
- [26] H.H. Asatryan, H.M. Asatrian, C. Greub and M. Walker, Phys. Lett. B **507**, 162 (2001).
- [27] B. Lange and M. Neubert, Nucl. Phys. B **690**, 249 (2004); [Errat.-ibid. B **723**, 201 (2005)].
- [28] M. Beneke and Th. Feldmann, Nucl. Phys. B **685**, 249 (2004).

- [29] A. Ali and A.S. Safir, Eur. Phys. J. C **25**, 583 (2002).
- [30] Particle Data Group, S. Eidelman *et al.*, Phys. Lett. B **592**, 1 (2004).
- [31] CDF Collaboration, D0 Collaboration and the Tevatron Electroweak Working Group, hep-ex/0507091.
- [32] P. Gambino, M. Gorbahn and U. Haisch, Nucl. Phys. B **673**, 238 (2003).
- [33] M. Gorbahn and U. Haisch, Nucl. Phys. B **713**, 291 (2005).
- [34] The Heavy Flavor Averaging Group, <http://www.slac.stanford.edu/xorg/hfag/> (Winter 2005 averages).
- [35] P. Ball and R. Zwicky, hep-ph/0510338.
- [36] S. J. Lee and M. Neubert, Phys. Rev. D **72**, 094028 (2005).
- [37] A.G. Grozin and M. Neubert, Phys. Rev. D **55**, 272 (1997).
- [38] P. Ball and R. Zwicky, Phys. Rev. D **71**, 014029 (2005).
- [39] A. Ali and A.Y. Parkhomenko, Eur. Phys. J. C **23**, 89 (2002); A. Ali, E. Lunghi and A.Y. Parkhomenko, Phys. Lett. B **595**, 323 (2004).
- [40] S.W. Bosch and G. Buchalla, Nucl. Phys. B **621**, 459 (2002).
- [41] B. Aubert *et al.* [BABAR Collaboration], hep-ex/0507003.
- [42] G. Burdman, Phys. Rev. D **57**, 4254 (1998).